MASTERARBEIT / MASTER'S THESIS

Titel der Masterarbeit / Title of the Master's Thesis

Emergent cosmological spacetime on a deformed Lorentzian fuzzy sphere

verfasst von / submitted by

Veronika Leonie Bachleitner, BSc

angestrebter akademischer Grad / in partial fulfilment of the requirements for the degree of

Master of Science (MSc)

Wien, 2022 / Vienna, 2022

Studienkennzahl lt. Studienblatt / degree programme code as it appears on the student record sheet:	A 066 876
Studienrichtung lt. Studienblatt / degree programme as it appears on the student record sheet:	Masterstudium Physik
Betreut von / Supervisor:	Mag. Harold Steinacker, PhD

Abstract

We construct a deformed Lorentzian fuzzy sphere as a toy model of a non-commutative cosmology with emergent singularities which appear in the semi-classical limit. The Laplacian on the Lorentzian fuzzy sphere does not agree with the Laplacian on the standard sphere. This leads to a modified scalar field propagator for the scalar field theory in the commutative limit. The induced metric on the Lorentzian fuzzy sphere does not agree with the standard metric on the sphere and we find a signature change around the poles of the sphere. We show how the singularities on the deformed Lorentzian fuzzy sphere and the corresponding scalar field propagator behave for different deformation parameters.

Zusammenfassung

Wir konstruieren eine deformierte Lorentzsche Fuzzy Sphäre als Modell einer nicht-kommutativen Kosmologie mit emergenten Singularitäten im semi-klassischen Limes. Der Laplace-Operator auf der Lorentzschen Fuzzy Sphäre ist nicht derselbe wie der Laplace-Operator auf der Standard Sphäre. Das führt zu einem modifizierten Skalarfeldpropagator für die skalare Feldtheorie im kommutativen Limes. Die induzierte Metrik auf der Lorentschen Fuzzy Sphäre ist nicht dieselbe wie die übliche Metrik auf der Sphäre und wir finden einen Signaturwechsel bei den Polen der Sphäre. Wir zeigen das Verhalten der Singularitäten auf der deformierten Lorentschen Fuzzy Sphäre und des Skalarfeldpropagators für verschiedene Deformationsparameter.

Acknowledgements

I thank my supervisor Mag. Harold Steinacker, PhD for his unending patience and for multiple discussions that were not only educational but also entertaining.
I also thank my father Mag. Johann Bachleitner for encouraging my endless questions about the universe in my childhood. None of us expected me to study physics; that decision must have been an emergent phenomenon.

Contents

1 Introduction

1.1 Motivation

Historically, Western philosophy and science has long believed space and time to be independent of other physical objects; they were absolute, the backdrop to our experienced reality. We had the presumption that space and time are not influenced by and do not influence our 'world'. It were most notably Hume and Mach who put this paradigm into question for us. [1]

With Einstein and the theory of relativity it became clear that time and space are not absolute frameworks and that we do not live in a fixed box of absolute space and time coordinates. Moreover, space and time are interdependent, now commonly known as spacetime, and the Einstein equations display the relationship between spacetime (geometry) and matter.

This was already one of the biggest changes of worldview as is. But why stop there? Why should this be all that we got wrong about our understanding of space/time? What else should we be rethinking?

Thus the first very simplistic motivation for fuzzy physics is this:

We know from quantum mechanics that at very small scales some physical elements are quantized. We've learned that space and time are not the presumed unchangeable backdrop on which all other phenomena take place but that both are interwoven with each other and play a part in cosmic storytelling. In conclusion spacetime is part of the physical reality. If we let that sink in for a moment we must allow ourselves to also consider spacetime to be quantized. And that's simply because it *could* be and we don't want to unnecessarily put ourselves into a paradigm box yet again.

Ydri [2] argues qualitatively that forming a relationship between the Heisenberg principle and the Einstein equations will result in quantized spacetime:

Following the Heisenberg principle the measurement of a coordinate point requires a momentum uncertainty which is the dependent on the accuracy of the measurement and, therefore, energy. But the Einstein equations tell us that matter/energy is coupled to geometry, in other words: superposition of matter means superposition of geometries [3].

What would it mean for spacetime to be quantized? Basically it suggests that there is a fundamental length scale where it is impossible to precisely measure time and space coordinates. What scale are we talking about? We already know from the study of quantum field theory that there is a fundamental length scale of the order of the Planck scale [4]: This scale with time intervals around $10^{-43}s$ and lengths around $10^{-35}m$ is associated with the unification of the fundamental interactions because at this scale gravity becomes comparably strong to the other interactions. Instead of assuming that at this scale something magical happens, we can hypothesize that the Planck scale itself – the lengths and times – are fundamental.

Analogous to how quantization in quantum mechanics is achieved by expressing functions as operators and implementing commutation relations between them we can elevate each (time/space) coordinate to be an operator and formulate commutation relations between the coordinate operators. These commutation relations naturally introduce the desired fundamental length scale because it becomes impossible to measure the position of a particle exactly when the space coordinates cannot be simultaneously diagonalised. [5] A field theory formulated on a fuzzy space is therefore already regularized (if compatible with the right symmetry group), i.e., the number of independent states per ("classical") unit volume is finite [4][6]. This is also a technical reason for the use of non-commutative geometry.

However, this hope to eliminate the ultraviolet divergences that arise in the conventional formulation of quantum field theory has led to more difficulty, namely the UV/IR (ultraviolet/infrared) mixing: Imposing a UV cutoff via non-commutative geometry results in IR divergences. [5][7]

Another motivation is that we might already come to the notion of non-commutative geometry purely by thinking about our understanding of relativity theory alone: we're aware that the universe looks different depending on where you are; i.e. it matters whether or not you are accelerated with respect to another observer or whether you are in a gravitational field. With non-commutative geometry we can put this on an even more fundamental level: the idea is it's not the existence of acceleration/gravity that is fundamental, but instead that on very small scales *any* change or measurement of position on spacetime is relevant. The naive picture which might help to visualise the concept of non-commutative geometry is to imagine that when you move one Planck-scale amount of length to the side then the geometry, hence also matter, changes with you (in actuality the notion of localisation vanishes entirely) – but as you leave the Planck scale and get closer to classical length scales the overall geometry will emerge from this non-commutative geometry.

More information on the historical motivations behind using non-commutative spaces in physics can be found in [8].

It is (for now) a question of taste whether one views spacetime at a fundamental length scale as discrete (a "lattice") or indeterminate in the sense of Heisenberg's uncertainty principle with the loss of any notion of a "point". In any case we will call this feature "fuzzy".

We will get to a more technical understanding in the next chapter. For now we are satisfied with knowing that by using this approach the quantum nature of reality is already embedded in the *geometry* of the fundamental model and that gravity, because it is fundamentally coupled to geometry, naturally emerges as you get further away from the Planck scale.

Let me just spend a moment on my own motivation, which is easily explained by the following observation: For years I did not realise that I misheard the lyrics to a song [1] (a song which actually never talked about "gravity"). My version goes like this:

And I would give all this and heaven too
I would give it all if only for a moment
That I could just understand the meaning of gravity
'Cause I've been scrawling it forever, but it never makes sense to me at all

The song (truly) ends with the line *"and I was screaming out a language that I never knew existed before"* which is precisely what happened in this thesis. Now let me walk you through this language.

1.2 Quantization

In theoretical physics we use different ways of quantizing a classical theory. Best known is probably canonical quantization. Here we are more interested in geometrical quantization because this is coordinate-free and appropriate also for phase spaces which aren't flat. [9]

In order to easily jump between the classical and quantum systems we construct a quantization map. In general a quantization map assigns to each mathematical object of the quantum system an appropriate mathematical object of the classical system. In our case this will mean that we can identify *elements of the matrix algebra* of the quantum system with *functions* of the classical system.

Someone using a quantization map may want to use it to quantize an already known classical system. We start the other way around, with the matrix algebra (i.e. with the quantum system), because we are looking for an underlying structure that is quantum in nature which will then reduce to a classical system in the limit. In this thesis we discuss the semi-classical limit, that is, the leading classical approximation of the non-commutative geometry in which the commutators are replaced with Poisson brackets [3].

[1] Florence + The Machine, "All This And Heaven Too"

We are satisfied with the semi-classical limit because we can already see the emerging structure there. Methods of how to get to the classical system (Star Products, Coherent States) can be found e.g. in [10], [11].

Let's get into the technical part.

First, we need a Poisson manifold $(\mathcal{M}, \{,.,\})$ — this is a manifold $\mathcal{M}$ equipped with a Poisson structure $\{,.,\}$. A Poisson structure on $\mathcal{M}$ is a bilinear map

$$\{.,.\} : \mathcal{C}(\mathcal{M}) \times \mathcal{C}(\mathcal{M}) \to \mathcal{C}(\mathcal{M}) \tag{1}$$

which satisfies antisymmetry, the Leibniz rule and the Jacobi identity.

A quantization map may be defined as follows:

Definition: Let $\mathcal{P}$ be a Poisson manifold. A quantization map is a linear map

$$\mathcal{Q} : \mathcal{C}(\mathcal{P}) \to \mathrm{End}(\mathcal{P}) \tag{2}$$

satisfying the axioms

- $\mathcal{Q}(1) = \mathbb{I}$
- $\mathcal{Q}(f)^\dagger = \mathcal{Q}(f^*) \quad \forall f \in \mathcal{C}(\mathcal{P})$
- *the correspondence principle:* (κ is the scale / quantization parameter)
  $\lim\limits_{\kappa\to 0} \frac{1}{\kappa}\left([\mathcal{Q}(f), \mathcal{Q}(g)] - i\mathcal{Q}(\{f,g\})\right) = 0 \quad \forall f, g \in \mathcal{C}(\mathcal{P})$
  $\lim\limits_{\kappa\to 0} \left(\mathcal{Q}(fg) - \mathcal{Q}(f)\mathcal{Q}(g)\right) = 0 \quad \forall f, g \in \mathcal{C}(\mathcal{P})$
- *irreducibility:*
  If $\{f_i, g\} = 0 \quad \forall i \in I$ implies $g \propto 1$
  then $[\mathcal{Q}(f_i), A] = 0 \quad \forall i \in I$ implies $A \propto 1$

The Poisson manifold can be directly associated to a Lie group[2] G: A symmetry of the system $\mathcal{P}$ is an element g of a Lie group G which acts symplectically on $\mathcal{P}$. [9] This may look like a lot right now but we will learn more about this in the course of the thesis as we need it. For an in-depth discussion of the mathematical structures see e.g. [12], [13].

In particular, quantization of the two-sphere S^2 leads to representations of the Lie group $SU(2)$. The symmetries of the quantized two-sphere are realised as the Lie algebra $su(2)$ which is well-known in quantum mechanics. We will see this play out once we make the construction of our modified fuzzy sphere in Chapter 2.

To prepare us for this we will now review the construction of the fuzzy sphere S_N^2.

1.3 Mathematical formulation of the fuzzy sphere S_N^2

The general idea is the following: We may construct a fuzzy space as a manifold equipped with a finite-dimensional matrix algebra which approximately reduces to the infinite dimensional algebra of functions in the commutative limit [4]. We choose a Lie algebra because these immediately give the right symmetry conditions and are equipped with natural derivations (vector fields) [6]. They have a symplectic form and resemble the already well-known quantum phase spaces [5]. The spacetime coordinates are the generators of the algebra, i.e. linear operators on irreducible representations of the Lie group.

Let's see now how that works for the two-sphere.

[2] for some notes on Poisson manifolds, Lie groups and Lie algebras see the Appendix 7

We know that the standard two-sphere S^2 with radius $\bar{r}$ [3] is a two-dimensional compact manifold defined by the set of points $(\bar{x}_1, \bar{x}_2, \bar{x}_3)$ of $\mathbb{R}^3$ which satisfy:

$$\bar{x}_1^2 + \bar{x}_2^2 + \bar{x}_3^2 = \bar{r}^2 \tag{3}$$

An algebra on this sphere is commutative with respect to pointwise multiplication of functions. One can choose the spherical harmonics Y_{lm} as a basis for this algebra.

The fuzzy sphere S_N^2 [2][3][5][10] is a quantization of the standard two-sphere S^2 with a cutoff in angular momentum. As we quantize the coordinates $(\bar{x}_1, \bar{x}_2, \bar{x}_3)$ to operators on a Hilbert space we choose to write them as matrices $Mat(N, \mathbb{C})$ in the adjoint representation of the Lie group $SU(2)$. This is why we say we are working with matrix algebras; matrices are at the basis of all fuzzy spaces. The cutoff in angular momentum is realised via a cutoff in the spherical harmonics.

The quantization map $\mathcal{Q}$ between S^2 and S_N^2 is then given by

$$\mathcal{Q} : \mathcal{C}(S^2) \to Mat(N, \mathbb{C}) \tag{4}$$

$$\bar{x}^a \mapsto \bar{X}^a = \kappa J^a \tag{5}$$

$$Y_m^l \mapsto \begin{cases} \bar{Y}_m^l & l < N \\ 0 & l \geq N \end{cases} \tag{6}$$

This reads as follows:

In the first line, Eq. (4), we say that: The quantization map $\mathcal{Q}$ maps the space of smooth functions on the sphere S^2 to the space of $N \times N$ dimensional complex matrices.

The Lie group $SU(N)$ consists precisely of these matrices:

$$SU(N) := \{A \in Mat(N, \mathbb{C}); AA^\dagger = \mathbb{I}, \det(A) = 1\} \tag{7}$$

Their dimension is

$$\dim(SU(N)) = N^2 - 1 \tag{8}$$

and the corresponding Lie algebra is

$$su(N) := \{A \in gl(N, \mathbb{C}); A^\dagger = -A, \mathrm{Tr}(A) = 0\} \tag{9}$$

In the second line of the quantization map, Eq. (5), we read: The coordinates $\bar{x}^a$ map to the matrices $\bar{X}^a$ which are chosen such that $\bar{X}^a = \kappa J^a$. $\kappa \in \mathbb{R}$ is a constant. J^a are the well-known generators of $su(2)$ in the N-dimensional irreducible representation. You may also know them as angular momentum operators.

These satisfy [4]

$$[J^a, J^b] = i\epsilon_{abc} J^c \tag{10}$$

The last line, Eq. (6) furthermore tells us that: The spherical harmonics Y_m^l map to the so-called *fuzzy* spherical harmonics $\bar{Y}_m^l$ which have a cutoff at $l = N$.

[3] In this subchapter most variables will have a bar on top in order to distinguish them from the variables used throughout the rest of the thesis.

[4] Indices in this section are raised and lowered with the Euclidean metric, therefore we don't really care whether they are up or down – yet. Don't worry about it until the next chapter.

We do know more about the angular momentum operators which are used in the construction of the matrices and can therefore read off even more information from the quantization map.

The quadratic Casimir operator $\vec{J}^2$ [5] is given by

$$\vec{J}^2 := J_1^2 + J_2^2 + J_3^2 \tag{11}$$

for $su(2)$ and commutes with all generators:

$$[\vec{J}^2, J^a] = 0 \tag{12}$$

The eigenvalue to $\vec{J}^2$ for some eigenvector v_λ is $l(l+1)$:

$$\vec{J}^2 v_\lambda = l(l+1) v_\lambda \tag{13}$$

where $l = 0, 1, 2, ..., N$

By Schur's Lemma, $\vec{J}^2$ must also be a multiple of the identity matrix:

$$\vec{J}^2 = c_R \mathbb{I} \tag{14}$$

The constant c_R depends only on the irreducible representation. Here it is

$$\vec{J}^2 = \frac{1}{4}(N^2 - 1)\mathbb{I} \tag{15}$$

This knowledge helps us to find a constraint to the fuzzy sphere:

$$(\bar{X}^1)^2 + (\bar{X}^2)^2 + (\bar{X}^3)^2 = \kappa^2 (J_1^2 + J_2^2 + J_3^2) = \kappa^2 \frac{1}{4}(N^2 - 1)\mathbb{I} \tag{16}$$

We can choose to fix the constant κ^2 to be a useful multiple of the constant radius of the sphere

$$\kappa^2 = \frac{\bar{r}^2}{c_R} = \bar{r}^2 \frac{4}{N^2 - 1} \tag{17}$$

such that

$$(\bar{X}^1)^2 + (\bar{X}^2)^2 + (\bar{X}^3)^2 = \bar{r}^2 \mathbb{I} \tag{18}$$

And hooray, this fits perfectly with what we know to be true for the classical two-sphere S^2: In view of the quantization map it is clear that Eq. (18) goes to Eq. (3) in the commutative limit!

This commutative limit is obviously given for $N \to \infty$ (where we would return to the 'usual', not the fuzzy, spherical harmonics). But not only that: Notice that the commutative limit can also be reached by letting $\kappa \to 0$

$$\kappa \bar{r} = \frac{\bar{r}^2}{\sqrt{c_R}} = \frac{2\bar{r}^2}{\sqrt{N^2 - 1}} \to 0 \tag{19}$$

[5] A Casimir operator, sometimes called Casimir invariant, can be formed for any Lie algebra and is a polynomial out of the generators that commutes with all generators.

which makes the parameter κ assume the role of Planck's constant $\hbar$ for the spacetime structure [6].

Going back to the quantization map we see that the generators $\bar{X}^a$ of the algebra $Mat(N, \mathbb{C})$ satisfy the commutation relations

$$[\bar{X}^a, \bar{X}^b] = i\epsilon_{abc}\kappa\bar{X}^c \tag{20}$$
$$\tag{21}$$

where $a = 1, 2, 3$.

We can now confidently call $\bar{X}^a$ the generators of the fuzzy sphere. We can interpret eigenvalues of $\bar{X}^a = \kappa\bar{J}^a$ as the fuzzy points on the fuzzy sphere. [6] The operators $\bar{X}^a$ [6] are a quantization of the coordinate functions $\bar{x}^a$ in the Euclidean space $\mathbb{R}^3$:

$$\bar{X}^a = \mathcal{Q}(\bar{x}^a): \quad S^2 \hookrightarrow \mathbb{R}^3 \tag{22}$$

This says essentially the same as the first two lines Eq. (4) and Eq. (5) of the quantization map above.

The algebra $Mat(N, \mathbb{C})$ can be decomposed into irreducible representations under the adjoint action of su(2):

$$\begin{aligned} Mat(N, \mathbb{C}) &\approxeq \mathbb{C}^N \otimes \mathbb{C}^N && (23)\\ &= (1) \oplus (3) \oplus \cdots \oplus (2N-1) && (24)\\ &= \{\bar{Y}_0^0\} \oplus \cdots \oplus \{\bar{Y}_m^{N-1}\} && (25)\end{aligned}$$

which is another way of putting the last line, Eq. (6), of the quantization map. These are the definitions for the fuzzy sphere you will most often find.

The Laplacian Δ on the fuzzy sphere is the same as for the usual sphere:

$$\Delta = \frac{1}{\sin^2\theta}\partial_\varphi^2 + \frac{1}{\sin\theta}\partial_\theta(\sin\theta\partial_\theta) \tag{26}$$

It has the solutions

$$\begin{aligned} \Delta\bar{Y}_m^l(\theta, \varphi) &= l(l+1)\bar{Y}_m^l && (27)\\ J^3\bar{Y}_m^l(\theta, \varphi) &= m\bar{Y}_m^l && (28)\\ & && (29)\end{aligned}$$

where the eigenvectors are the spherical harmonics. We have $l = 0, 1, 2, ...$ and $m = -l, ..., +l$ for the usual sphere; however, in the fuzzy case the spherical harmonics $\bar{Y}_m^l$ have a cutoff at $l = N$.

The fuzzy spherical harmonics satify the orthonormalization condition:

$$\int_{S^2} \frac{d\Omega}{4\pi} \bar{Y}_{lm}^*(\theta, \varphi)\bar{Y}_{l'm'}(\theta, \varphi) = \delta_{ll'}\delta_{mm'} \tag{30}$$

[6] Why do I sometimes call $\bar{X}^a$ operators and sometimes generators? The name "generator" refers to their nature as generators of the algebra, which is also what we call J^a, the "generators of angular momentum". The name "operator" relates to the usual language of quantization where we say that we map classical observables to quantum operators. So $\bar{X}^a$ are the generators of the fuzzy sphere but also operators.

and we can use a linear combination expansion:

$$\bar{f}(\theta,\varphi) = \sum_{l=0}^{N}\sum_{m=-l}^{+l} \bar{f}_{lm}\bar{Y}_{lm}(\theta,\varphi) \tag{31}$$

$$\bar{f}_{lm} = \int_{S^2} \frac{d\Omega}{4\pi}\bar{Y}^*_{lm}(\theta,\varphi)\bar{f}(\theta,\varphi) \tag{32}$$

Let's take a quick look at a bit of physics on the fuzzy sphere as well: A simple, free Euclidean action for a scalar field on the fuzzy sphere can look like

$$S_F = \mathrm{Tr}\left(-\frac{1}{2}[\bar{X},\bar{f}][\bar{X},\bar{f}] + \frac{\bar{\mu}^2}{2}\bar{f}\right) \tag{33}$$

We recall a property of the trace and the quantization condition involving the trace:

$$\mathrm{Tr}\left([\bar{X},\bar{f}][\bar{X},\bar{f}]\right) = -\,\mathrm{Tr}\left(\bar{f}[\bar{X},[\bar{X},\bar{f}]\right) \tag{34}$$

$$\mathrm{Tr}\left(\mathcal{Q}(f)\right) = \frac{1}{2\pi}\int_{S^2}\Omega\bar{f} \tag{35}$$

These together with the symplectic form Ω providing the integration measure allow us to rewrite the action in terms of the Laplacian Δ

$$S_F = k\int_{S^2}\left(-\frac{1}{2}\bar{f}(\theta,\varphi)\Delta\bar{f}(\theta,\varphi) + \frac{\bar{\mu}^2}{2}\bar{f}(\theta,\varphi)\right) \tag{36}$$

where k is some constant that takes on different values depending on definitions.

We can now plug in the linear combination expansion of $\bar{f}(\theta,\varphi)$ (Eq. (32)) into fuzzy spherical harmonics and evaluate the Laplacian to find the action expressed in terms of the eigenmodes:

$$S_F = \sum_{l,m}^{n+1} \frac{|\bar{f}^2_{lm}|}{2}(l(l+1)+\bar{\mu}^2) \tag{37}$$

These steps will be done more rigorously for the modified fuzzy sphere that is subject to this thesis. Here we have simply established the preexisting framework and we can now dive into the principal part of the thesis. In the following chapter I will construct a specific version of a deformed fuzzy sphere living on a Minkowski metric. I will closely follow the procedure outlined above.

2 Construction of a deformed Lorentzian fuzzy sphere

Matrix models and especially the fuzzy sphere as a basic example have been investigated in various ways, i.e. constructing quantum field theories on these spaces. [14]

The next step has been to investigate matrix models and more specifically fuzzy spaces with Lorentzian signature. The beauty in these models is that gravity appears as an emergent effect of the underlying quantum spacetime [15]. It has been shown that a suitable action on some Lorentzian fuzzy spaces lead in the commutative limit to solutions which can be interpreted as cosmologies with big bang singularities [16] [17]. One such space will be constructed here.

2.1 Action and equations of motion

Let us start our adventure with the action

$$S(X) = \frac{1}{g}\operatorname{Tr}\left(\frac{1}{4}\eta_{\mu\mu'}\eta_{\nu\nu'}[X^{\mu'},X^{\nu'}][X^{\mu},X^{\nu}] - \frac{\mu^2}{2}X_iX^i + \frac{\mu_0^2}{2}X_0X^0\right) \tag{38}$$

The action is chosen similarly to the action S_F that we've previously seen for the standard fuzzy sphere in Eq. (33). However, we now use the Minkowski metric tensor in $2+1$ dimensions with

$$(\eta_{\mu\nu}) = \operatorname{diag}(-1,1,1) \tag{39}$$

the indices are $\mu,\nu = 0,1,2$ and $i,j = 1,2$ and we use $\eta_{\mu\nu}$ to raise and lower indices.

Another difference is that we now have two terms which could potentially be identified as a kind of "mass" term. Right away we want to distinguish between possibly "space"-type operators, X_1, X_2, and a possibly "time"-type operator X_0. Each kind has their own "mass"-like parameter. Keep in mind that this is but an explanation for the reason we chose this kind of action and immediately forget these physical terms of describing the action. A priori we cannot identify anything that should be called "mass", "timelike", "spacelike" or anything else like this. We will however stick to calling Eq. (38) an action and proceed to find the equations of motion (after all, we want to *find* something physical in the end and conveniently choose a physicist's path of calculations).

The equations of motion can be found by varying the action. We will explicitly write down the following calculation:

$$0 = d\operatorname{Tr}\left([X^a,X^b][X_a,X_b]\right) = 2\operatorname{Tr}\left(d[X^a,X^b][X_a,X_b]\right) = \tag{40}$$

$$4\operatorname{Tr}\left([dX^a,X^b][X_a,X_b]\right) = 4\operatorname{Tr}\left(dX^a[X^b,[X_a,X_b]]\right) \tag{41}$$

$$\tag{42}$$

where for the last line we use the identity

$$\operatorname{Tr}([A,B][C,D]) = Tr(A[B,[C,D]]) \tag{43}$$

We also know that

$$\operatorname{Tr}(AB) = 0\ \forall A \implies B = 0 \tag{44}$$

and find that

$$[X_a,X_b] = 0 \tag{45}$$

With this in mind it is easy to see that the equations of motion are:

$$-[X_\mu, [X^\mu, X^i]] - \mu^2 X^i = 0 \tag{46}$$

$$-[X_\mu, [X^\mu, X^0]] + \mu_0^2 X^0 = 0 \tag{47}$$

This is our preliminary investigation of the action Eq. (38) which will give us important information later.

2.2 Generators

We are on a sphere and therefore comfortably choose the generators of $SU(2)$

$$\boxed{[J_i, J_j] = i\epsilon_{ijk} J_k} \tag{48}$$

to define the matrices

$$\boxed{X_0 := \omega_{(0)} J_3,\ X_1 := \omega_{(1)} J_1,\ X_2 := \omega_{(2)} J_2} \tag{49}$$

where $\omega_{(\mu)} \in \mathbb{R}$.

The generators of $SU(2)$ should be well-known to readers as the angular momentum operators; they are explained in more detail in the appendix 7.

Apart from the fact that we use a Minkowski instead of Euclidean signature the definition given by Eq. (49) is the second main difference from the standard fuzzy sphere: the three generators X_μ differ according to the choice of $\omega_{(\mu)}$.

A word on notation: The bracketed indices of $\omega_{(\mu)}$ are not to be summed over, hence the round brackets, but they change according to the corresponding change of the usual indices on the matrices. It might take a moment to get used to this notation. It is a trick that enables me to do general calculations instead of having to do them separately for each possible choice of coordinate combinations. It becomes easier to read once you realise that the constants $\omega_{(...)}$ "stick" with their accompanying matrices by changing index with them.
Example: $\omega_{(\mu)} X_\mu \delta^{\mu\nu} = \omega_{(\nu)} X_\nu$, where we've summed over the indices of the matrix X_μ and $\delta^{\mu\nu}$ to get X_ν and have manually changed the bracketed index of the constant $\omega_{(\mu)}$ to $\omega_{(\nu)}$) because we know that the index of the matrix is now ν.
In summary: the constants have indices in round brackets which are not summed over; they keep track of the matrix that the constant belongs to.

We choose

$$\boxed{\omega_{(1)}^2 = \omega_{(2)}^2 = \omega^2} \tag{50}$$

to implement rotational invariance. This remains true for the rest of the calculations.

Calculating the individual commutators in terms of the X_μ matrices, e.g. $[X_0, X_1] = i\frac{\omega_{(0)}\omega_{(1)}}{\omega_{(2)}} X_2$,, we generally find

$$\boxed{[X_\mu, X_\nu] = i\epsilon_{\mu\nu\rho} \frac{\omega_{(\mu)}\omega_{(\nu)}}{\omega_{(\rho)}}\ X_\rho} \tag{51}$$

This is the first exercise of reading my index notation: The omegas in the numerator carry the same greek index as the matrices on the left side of the equation. The omega in the denominator belongs to the matrix X_ρ on the right side of the equation. According to the definition Eq. (49) this is exactly as it should be.

We now go on to the more difficult task of calculating the double bracket. In the following calculation we will use lowered indices only. We implement the metric tensor $\eta_{\mu\nu}$ in the next step; for now it is enough to try to understand how the indices behave without worrying about the metric.

$$
\begin{aligned}
[X_\alpha, [X_\mu, X_\nu]] &= i\frac{\omega_{(\mu)}\omega_{(\nu)}}{\omega_{(\rho)}} [X_\alpha, \epsilon_{\mu\nu\rho} X_\rho] && (52)\\
&= i^2 \frac{\omega_{(\mu)}\omega_{(\nu)}}{\omega_{(\rho)}} \frac{\omega_{(\alpha)}\omega_{(\rho)}}{\omega_{(\sigma)}} \epsilon_{\alpha\rho\sigma}\epsilon_{\mu\nu\rho} X_\sigma && (53)\\
&= -\frac{\omega_{(\mu)}\omega_{(\nu)}\omega_{(\alpha)}}{\omega_{(\sigma)}} \left(\delta_{\alpha\mu}\delta_{\sigma\nu} - \delta_{\alpha\nu}\delta_{\sigma\mu}\right) X_\sigma && (54)\\
&= \left(\omega_{(\mu)}\omega_{(\alpha)}\delta_{\alpha\mu}X_\nu - \omega_{(\nu)}\omega_{(\alpha)}\delta_{\alpha\nu}X_\mu\right) && (55)\\
& && (56)
\end{aligned}
$$

Something interesting happens from the third to the last line: When we evaluate $\delta_{\sigma\nu}$ and $\delta_{\sigma\mu}$ the bracketed indices of the omegas change as well and cancel out.

We can now apply the metric tensor $\eta_{\mu\nu}$:

$$
\begin{aligned}
[X_\mu, [X^\mu, X^\nu]] &= \eta_{\mu\alpha}[X^\alpha, [X^\mu, X^\nu]] && (57)\\
&= \eta_{\mu\alpha}\left(\omega_{(\mu)}\omega_{(\alpha)}\delta^{\alpha\mu}X^\nu - \omega_{(\nu)}\omega_{(\alpha)}\delta^{\alpha\nu}X^\mu\right) && (58)\\
&= \eta^\mu_\mu\, \omega^2_{(\mu)}X^\nu - \eta^\nu_\mu\, \omega^2_{(\nu)}X^\mu && (59)\\
&= -\omega^2_{(0)}X^\nu + 2\omega^2 X^\nu + \delta_{\nu 0}\omega^2_{(0)}X^0 - \delta_{\nu i}\omega^2 X^i && (60)\\
& && (61)
\end{aligned}
$$

We can now distinguish two cases:

$$\boxed{[X_\mu, [X^\mu, X^i]] = \left(\omega^2 - \omega^2_{(0)}\right) X^i} \quad (62)$$

$$\boxed{[X_\mu, [X^\mu, X^0]] = 2\omega^2 X^0} \quad (63)$$

We can put these into the equations of motion Eq. (47) which we've found for the action Eq. (38) before. We find:

$$
\begin{aligned}
[X_\mu, [X^\mu, X^i]] + \mu^2 X^i &= \left(\omega^2 - \omega^2_{(0)} + \mu^2\right) X^i = 0 && (64)\\
[X_\mu, [X^\mu, X^0]] - \mu_0^2 X^0 &= (2\omega^2 - \mu_0^2)X^0 = 0 && (65)
\end{aligned}
$$

and this gives us a constraint for the constants ω and $\omega_{(0)}$:

$$\boxed{\implies \omega^2 = \frac{1}{2}\mu_0^2} \quad (66)$$

$$\boxed{\implies \omega^2_{(0)} = \frac{1}{2}(\mu_0^2 + 2\mu^2)} \quad (67)$$

$\mu^2 = \omega_{(0)}^2 - \frac{1}{2}\mu_0^2$ means that, in order to let $\mu \in \mathbb{R}$, $\omega_{(0)}^2 > \frac{1}{2}\mu_0^2$ and thus

$$\boxed{\omega_{(0)}^2 > \omega^2} \tag{68}$$

2.3 Casimir and eigenvalues

Let's remember that we've based this on the generators of $SU(2)$ and that we can learn a lot from our understanding of $SU(2)$.

We can relate the X_μ's to the quadratic Casimir by

$$\omega^2 \vec{J}^2 \tag{69}$$

$$= \frac{\omega^2}{\omega_{(0)}^2}\, \omega_{(0)}^2 (J_3)^2 + \omega_{(1)}^2 (J_1)^2 + \omega_{(2)}^2 (J_2)^2 \tag{70}$$

$$= -\frac{\omega^2}{\omega_{(0)}^2} X_0 X^0 + X_1 X^1 + X_2 X^2 \tag{71}$$

where we've made use of the choice that $\omega_{(1)}^2 = \omega_{(2)}^2 = \omega^2$.

Keep in mind that indices are still raised and lowered with the Minkowski metric, and therefore we have a sign-change when we rewrite:

$$\frac{\omega^2}{\omega_{(0)}^2}(X_0)^2 + (X_1)^2 + (X_2)^2 = \omega^2 \vec{J}^2 \tag{72}$$

This is the constraint for our sphere.

We can use the $su(2)$ eigenvalue equations [18], where λ is an eigenvalue and v_λ an eigenvector, to find the eigenvalues for our matrices:

$$\vec{J}^2 v_\lambda = l(l+1) v_\lambda \tag{73}$$

$$X_0 v_{\lambda'} = m v_{\lambda'} \tag{74}$$

where $m = -l, ..., +l$ and $l = 0, 1, 2, ...$ This means that in our case,

$$\omega^2 \vec{J}^2\, v_\lambda = \omega^2 l(l+1)\, v_\lambda \tag{75}$$

$$X_0\, v_{\lambda'} = \omega_{(0)} m\, v_{\lambda'} \tag{76}$$

$$\tag{77}$$

where $m = -l, ..., +l$ and $l = 0, 1, 2, ..., N$.

We have now gathered enough information from the matrices and will try to find out how these translate to the semi-classical limit.

3 The semi-classical limit

We consider the semi-classical Euclidean sphere $S^2 \subset \mathbb{R}^{2,1}$ which carries a natural $SU(2)$-invariant Poisson structure. At the end of this chapter we will have a quantization map.

Carrying the matrix calculations over to the semi-classical realm I will replace the matrices X^μ by space-time commuting coordinates x^μ. x^0 denotes a time coordinate, x^i with $i = 1, 2$ denote space coordinates.

The constraint on the $su(2)$ Casimir operator (Eq. (72)) must be satisfied in the commutative limit as well:

$$\frac{\omega^2}{\omega_{(0)}^2} x_0^2 + x_1^2 + x_2^2 = \omega^2 R^2 \tag{78}$$

with a constant R that is yet to be determined. Note: Here indices are still raised/lowered via the Minkowski metric so that we see a change of sign in the following: $-\frac{\omega^2}{\omega_{(0)}^2} x_0 x^0 + x_1 x^1 + x_2 x^2 = \omega^2 R^2$. To avoid as much confusion as possible I will try to keep indices lowered and otherwise comment in the text. For now summation is obvious everywhere it occurs.

Next I need to replace the commutator of generators X^μ by a Poisson bracket of the functions of the coordinates x^μ. We found that the commutation relations of our operators with $i, j = \{1, 2\}$ are

$$[X_0, X_i] = i\epsilon_{0ij}\omega_{(0)} X_j \tag{79}$$

$$[X_i, X_j] = i\epsilon_{0ij} \frac{\omega^2}{\omega_{(0)}} X_0 \tag{80}$$

these are carried over to Poisson brackets with our semi-classical coordinates as follows:

$$\boxed{\{x_0, x_i\} = \epsilon_{0ij}\ \omega_{(0)} x_j} \tag{81}$$

$$\boxed{\{x_i, x_j\} = \epsilon_{ij0}\ \frac{\omega^2}{\omega_{(0)}} x_0} \tag{82}$$

where $i, j \in \{1, 2\}$.

With this we can realize the action of SU(2) on functions by the Hamiltonian vector fields acting on a function ϕ via the poisson bracket.

$$J_3 \triangleright \phi = \frac{i}{\omega_{(0)}} \{x_0, \phi\} \tag{83}$$

$$J_i \triangleright \phi = \frac{i}{\omega_{(i)}} \{x_i, \phi\} \tag{84}$$

The triangle $\triangleright$ is math symbolism for "acting on from the left". A group element, here J_3 and J_i, can act on some other object, here ϕ, and it acts on this object from the left or from the right. We distinguish between left action $\triangleright$ and right action $\triangleleft$ because things are non-commutative. You will see this again only in the appendix and in the referenced mathematics literature.

Explicitly, we can calculate:

$$J_3 \triangleright \phi = \frac{i}{\omega_{(0)}} \{x_0, \phi\} = \frac{i}{\omega_{(0)}} \epsilon_{0ij}\omega_{(0)} x_i \partial_j \phi = i\epsilon_{0ij} x_i \partial_j \phi \tag{85}$$

$$\tag{86}$$

$$J_i \triangleright \phi = \frac{i}{\omega_{(i)}} \{x_i, \phi\} = \frac{i}{\omega_{(i)}} \epsilon_{ij0}\ \frac{\omega^2}{\omega_{(0)}} x_j\ \partial_0 \phi + \frac{i}{\omega_{(i)}} \epsilon_{i0j}\ \frac{\omega^2}{\omega_{(0)}} x_0\ \partial_j \phi \tag{87}$$

$$= i\frac{\omega_{(i)}}{\omega_{(0)}} \epsilon_{ij0}\ \left(x_j \partial_0 \phi - x_0\ \partial_j \phi\right) \tag{88}$$

We will need these later but we will use them explicitely for spherical coordinates which makes it more comprehensible what they do. For now it's okay if they only seem like pretty, curly symbols.

Luckily we don't need to figure out a double action / double Poisson bracket at this stage and will do this later when we know which specific double Poisson brackets we need.

3.1 The Laplacian

We now want to build the Laplacian on this fuzzy sphere. Recall the quadratic Casimir on S^2 and rewrite it in terms of the semi-classical coordinates:

$$C^{(2)}\phi = \left(J_1^2 + J_2^2 + J_3^2\right)\phi \tag{89}$$

$$\approx \frac{1}{\omega^2}\{x_1, \{x_1, \phi\}\} + \frac{1}{\omega^2}\{x_2, \{x_2, \phi\}\} + \frac{1}{\omega_{(0)}^2}\{x_0, \{x_0, \phi\}\} \tag{90}$$

Notice that here, all terms have positive sign.
The Laplacian with respect to the embedding metric is defined as:

$$\Box_x\phi := -\{x_0, \{x_0, \phi\}\} + \{x_1, \{x_1, \phi\}\} + \{x_2, \{x_2, \phi\}\} \tag{91}$$

notice that there is one term with negative sign because of the metric.
We can plug Eq. (90) into the Laplacian:

$$\Box_x\phi := -\{x_0, \{x_0, \phi\}\} + \{x_1, \{x_1, \phi\}\} + \{x_2, \{x_2, \phi\}\} \tag{92}$$

$$= -\{x_0, \{x_0, \phi\}\} + \omega^2 C^{(2)}\phi - \frac{\omega^2}{\omega_{(0)}^2}\{x_0, \{x_0, \phi\}\} \tag{93}$$

$$\boxed{\Box_x\phi = \omega^2 C^{(2)}\phi - \left(1 + \frac{\omega^2}{\omega_{(0)}^2}\right)\{x_0, \{x_0, \phi\}\}} \tag{94}$$

The brackets in the extra term, $\{x_0, \{x_0, \phi\}\}$, are proportional to $J_3^2\phi$. In the following I will show what $\{x_0, \{x_0, \phi\}\}$ is in spherical coordinates.

3.2 Poisson Brackets in spherical coordinates

For a fuzzy sphere, of course, spherical coordinates are the obvious choice. The Poisson bracket on the sphere representing the coadjoint orbit for a given radius r is defined by

$$\{\theta, \theta\} = 0 \tag{95}$$

$$\{\varphi, \varphi\} = 0 \tag{96}$$

$$\{\theta, \varphi\} = -\{\varphi, \theta\} \tag{97}$$

We found the poisson brackets on the semiclassical fuzzy sphere on $\mathbb{R}^3$ in Eq. (82). For the individual coordinates they are:

$$\{x_0, x_1\} = \omega_{(0)}x_2 \tag{98}$$

$$\{x_2, x_0\} = \omega_{(0)}x_1 \tag{99}$$

$$\{x_1, x_2\} = \frac{\omega^2}{\omega_{(0)}}x_0 \tag{100}$$

For easier calculation we can now introduce new coordinates y_μ such that their Poisson bracket reads

$$\{y_\mu, y_\nu\} = \epsilon_{\mu\nu\rho} y_\rho \tag{101}$$

which means that we must define them as

$$y_\mu := \frac{1}{\omega_{(\mu)}} x_\mu \tag{102}$$

I want the y_μ to be spherical coordinates, so I choose:

$$\begin{aligned} y_1 &= r \sin\theta \cos\varphi \\ y_2 &= r \sin\theta \sin\varphi \\ y_0 &= r \cos\theta \end{aligned}$$

where $\theta \in [0, \pi], \varphi \in [0, 2\pi)$.

Note that, since the original operators X_μ were defined as $X_0 := \omega_{(0)} J_3$, $X_1 := \omega_{(1)} J_1$, $X_2 := \omega_{(2)} J_2$ we see that the y_μ coordinates are immediately related to angular momentum. This fixes r to the value:

$$\boxed{r = \sqrt{\frac{N^2 - 1}{4}}} \tag{103}$$

We can also show now that $R = r$ using the constraint on the Casimir:

$$\begin{aligned} \omega^2 R^2 &= \frac{\omega^2}{\omega_{(0)}^2} x_0^2 + x_1^2 + x_2^2 && (104) \\ &\frac{\omega^2}{\omega_{(0)}^2} \omega_{(0)}^2 r^2 \cos^2\theta + \omega^2 r^2 \sin^2\theta \cos^2\varphi + \omega^2 r^2 \sin^2\theta \sin^2\varphi && (105) \\ &= \omega^2 r^2 \cos^2\theta + \omega^2 r^2 \sin^2\theta && (106) \\ &= \omega^2 r^2 && (107) \end{aligned}$$

and therefore the constraint can also be written as

$$\frac{\omega^2}{\omega_{(0)}^2} x_0^2 + x_1^2 + x_2^2 = \frac{1}{4}(N^2 - 1)\omega^2 \tag{108}$$

Now that we can use spherical coordinates let's first evaluate $\{\frac{y_2}{y_1}, y_0\}$ using the Leibniz rule:

$$\{\frac{y_2}{y_1}, y_0\} = \frac{1}{y_1}\{y_2, y_0\} - \frac{y_2}{y_1^2}\{y_1, y_0\} = 1 - \frac{y_2}{y_1^2}(-y_2) = 1 + \frac{y_2^2}{y_1^2} \tag{109}$$

When we plug the spherical coordinates into Eq. (109) we find

$$\{\frac{\sin\varphi}{\cos\varphi}, r\cos\theta\} = \left(1 + \frac{\sin^2\varphi}{\cos^2\varphi}\right) = (1 + \tan^2\varphi) = \frac{1}{\cos^2\varphi} \tag{110}$$

We can also look at the relation

$$\boxed{\{f(\varphi), g(\theta)\} = \frac{\partial f}{\partial \varphi}\frac{\partial g}{\partial \theta}\{\varphi, \theta\}} \tag{111}$$

and put in $f(\varphi) = \tan\varphi, g(\theta) = r\cos\theta$ and find for this equation:

$$\{\tan\varphi, r\cos\theta\} = -\frac{1}{\cos^2\varphi} r\sin\theta\{\varphi, \theta\} \tag{112}$$

We can put Eq. (110) and Eq. (112) together and now see that

$$\boxed{\{\varphi, \theta\} = -\frac{1}{r\sin\theta}} \tag{113}$$

We can cross-check this by evaluating $\{y_0, y_1\}$ and $\{y_1, y_2\}$ with the use of this result. Keep in mind that $\{\varphi, \theta\} = -\{\theta, \varphi\}$.

$$\begin{aligned}
\{y_0, y_1\} &= \{r\cos\theta, r\sin\theta\cos\varphi\} \\
&= r^2\{\cos\theta, \cos\varphi\}\sin\theta \\
&= r^2(-\sin\theta)(-\sin\varphi)\{\theta, \varphi\}\sin\theta \\
&= r^2\sin^2\theta\sin\varphi\frac{1}{r\sin\theta} \\
&= r\sin\theta\sin\varphi \\
&= y_2
\end{aligned}$$

$$\begin{aligned}
\{y_1, y_2\} &= \{r\sin\theta\cos\varphi, r\sin\theta\sin\varphi\} \\
&= r^2\sin\theta\{\cos\varphi, \sin\theta\}\sin\varphi + r^2\cos\varphi\{\sin\theta, \sin\varphi\}\sin\theta \\
&= r^2\sin\theta(-\sin\varphi)\cos\theta\{\varphi, \theta\}\sin\varphi + r^2\cos\varphi\cos\theta\cos\varphi\{\theta, \varphi\}\sin\theta \\
&= r^2\sin\theta\cos\theta(-\sin^2\varphi)(-\frac{1}{r\sin\theta}) + \cos^2\varphi\cos\theta\sin\theta(\frac{1}{r\sin\theta}) \\
&= r\cos\theta \\
&= y_0
\end{aligned}$$

Works out! Therefore, when we look at the effect of the poisson brackets on a function $\phi(\theta, \varphi)$ we can use this result and immediately see that:

$$\begin{aligned}
\{r\cos\theta, \phi(\theta, \varphi)\} &= (-r\sin\theta)\{\theta, \varphi\}\partial_\varphi\phi && (114) \\
&= (-r\sin\theta)\frac{1}{r\sin\theta}\partial_\varphi\phi && (115) \\
&= -\partial_\varphi\phi && (116)
\end{aligned}$$

Of course this operation can be done twice:

$$\{r\cos\theta, \{r\cos\theta, \phi\}\} = \partial_\varphi^2\phi \tag{117}$$

Now recall the relationship between the y_μ and x_μ coordinates: $y_\mu = \frac{1}{\omega_{(\mu)}}x_\mu$. This means that we now have our additional term:

$$\boxed{\{x_0, \{x_0, \phi\}\} = \omega_{(0)}^2\partial_\varphi^2\phi} \tag{118}$$

and can be very happy.

3.3 Solutions to the Box-Operator Differential Equation

In Eq. (94) we found the corrected Laplacian for our model. We can now work with it because we know the explicit form of the extra-term accompanying it:

$$\Box_x \phi = \omega^2 C^{(2)} \phi - \left(1 + \frac{\omega^2}{\omega_{(0)}^2}\right) \{x_0, \{x_0, \phi\}\} \tag{119}$$

$$\approxeq \omega^2 \Box_g \phi - \left(1 + \frac{\omega^2}{\omega_{(0)}^2}\right) \omega_{(0)}^2 \partial_\varphi^2 \phi \tag{120}$$

We want to consider eigenfunctions of the form $\Box_x \phi = \Lambda \phi$:

$$\omega^2 \Box_g \phi - \left(1 + \frac{\omega^2}{\omega_{(0)}^2}\right) \{x_0, \{x_0, \phi\}\} = \Lambda \phi \tag{121}$$

$$\tag{122}$$

The first part of this equation is the usual spherical Laplace operator $\Box_g \phi$. We notice that the second term can be identified with $\omega_{(0)}^2$ times the J_3 operator acting twice on ϕ multiplied by the factor $\left(1 + \frac{\omega^2}{\omega_{(0)}^2}\right)$.

This means that we already have the following solutions:

The eigenvalue equation for an eigenvalue $\Lambda_{(1)}$

$$\omega^2 \Box_g \phi = \Lambda_{(1)} \phi \tag{123}$$

is solved by the fuzzy spherical harmonics $\bar{Y}_{lm}(\theta, \phi)$ (these are the same as the usual spherical harmonics but with a cutoff at $l = N$) and the eigenvalues $\omega^2 l(l+1)$ and $\omega^2 m$:

$$\omega^2 \Box_g \bar{Y}_{lm}(\theta, \phi) = \omega^2 l(l+1) \bar{Y}_{lm}(\theta, \phi) \tag{124}$$

$$\omega^2 J_3 \bar{Y}_{lm}(\theta, \phi) = \omega^2 m \bar{Y}_{lm}(\theta, \phi) \tag{125}$$

and the eigenvalue equation of the second term for an eigenvalue $\Lambda_{(2)}$

$$-\left(1 + \frac{\omega^2}{\omega_{(0)}^2}\right) \omega_{(0)}^2 J_3^2 \phi = \Lambda_{(2)} \phi \tag{126}$$

is actually the same as the J_3 solution above only multiplied by another factor, so the eigenvalue equation for the eigenvalue $\Lambda_{(2)}$ is solved again by fuzzy spherical harmonics

$$-\left(1 + \frac{\omega^2}{\omega_{(0)}^2}\right) \omega_{(0)}^2 J_3^2 \bar{Y}_{lm}(\theta, \phi) = -\left(1 + \frac{\omega^2}{\omega_{(0)}^2}\right) \omega_{(0)}^2 m^2 \bar{Y}_{lm}(\theta, \phi) \tag{127}$$

This means that the eigenvalue for the eigenvalue equation

$$\omega^2 \Box_g \phi - \left(1 + \frac{\omega^2}{\omega_{(0)}^2}\right) \{x_0, \{x_0, \phi\}\} = \Lambda \phi \tag{128}$$

$$\tag{129}$$

is given by

$$\boxed{\Lambda = \Lambda_{(1)} + \Lambda_{(2)} = \omega^2 l(l+1) - \left(\omega_{(0)}^2 + \omega^2\right) m^2} \tag{130}$$

with $l = 0, 1, 2, ..., N$ and $m = -l, ..., +l$

3.3.1 Solving the eigenvalue equation with spherical coordinates

We have a significant change to the standard eigenvalue solution, therefore we might want to try a second approach to verify the result. We are on a sphere after all so we can try to solve the differential equation

$$\Box_x \phi = \Lambda \phi \tag{131}$$

by hand with the use of spherical coordinates:

$$\begin{aligned}
\Box_x \phi &= \omega^2 \left(\frac{1}{\sin\theta} \partial_\theta (\sin\theta \partial_\theta \phi) + \frac{1}{\sin^2\theta} \partial_\varphi^2 \phi \right) - \left(1 + \frac{\omega^2}{\omega_{(0)}^2} \right) \omega_{(0)}^2 \partial_\varphi^2 \phi &(132)\\
&= \omega^2 \left(\frac{1}{\sin\theta} \partial_\theta (\sin\theta \partial_\theta \phi) + \frac{1}{\sin^2\theta} \partial_\varphi^2 \phi - \partial_\varphi^2 \phi \right) - \omega_{(0)}^2 \partial_\varphi^2 \phi &(133)\\
&= \omega^2 \left(\frac{1}{\sin\theta} \partial_\theta (\sin\theta \partial_\theta \phi) + \frac{1}{\tan^2\theta} \partial_\varphi^2 \phi \right) - \omega_{(0)}^2 \partial_\varphi^2 \phi &(134)
\end{aligned}$$

Because ϕ depends on two variables this calls for a separation ansatz:

$$\phi(\varphi, \theta) = f(\varphi) g(\theta) \tag{135}$$

in detail this looks as follows

$$\begin{aligned}
\Box_x \left(f(\varphi) g(\theta) \right) &= \omega^2 \left(\frac{1}{\sin\theta} \partial_\theta (\sin\theta \partial_\theta [f(\varphi) g(\theta)]) + \frac{1}{\tan^2\theta} \partial_\varphi^2 [f(\varphi) g(\theta)] \right) - \omega_{(0)}^2 \partial_\varphi^2 [f(\varphi) g(\theta)] &(136)\\
&= \omega^2 \left(\frac{f(\varphi)}{\sin\theta} \partial_\theta (\sin\theta \partial_\theta g(\theta)) + \frac{g(\theta)}{\tan^2\theta} \partial_\varphi^2 f(\varphi) \right) - \omega_{(0)}^2 g(\theta) \partial_\varphi^2 f(\varphi) &(137)\\
&= f(\varphi) \frac{\omega^2}{\sin\theta} \partial_\theta \left(\sin\theta \partial_\theta g(\theta) \right) + g(\theta) \left(\frac{\omega^2}{\tan^2\theta} - \omega_{(0)}^2 \right) \partial_\varphi^2 f(\varphi) &(138)
\end{aligned}$$

which then leads to the following equation where we omit the indication of variable dependencies for better readability:

$$\frac{1}{f} \Box_x (fg) = \omega^2 \left[\frac{1}{g} \frac{1}{\sin\theta} \partial_\theta \left(\sin\theta \partial_\theta g \right) + \frac{1}{f} \left(\frac{1}{\tan^2\theta} - \frac{\omega_{(0)}^2}{\omega^2} \right) \partial_\varphi^2 f \right] \tag{139}$$

This can again be rewritten:

$$\begin{aligned}
\frac{1}{f} \Box_x (fg) &= \omega^2 \left[\frac{1}{g} \frac{1}{\sin\theta} \left(\cos\theta \partial_\theta g + \sin\theta \partial_\theta^2 g \right) + \frac{1}{f} \left(\frac{1}{\tan^2\theta} - \frac{\omega_{(0)}^2}{\omega^2} \right) \partial_\varphi^2 f \right] &(140)\\
&= \omega^2 \left[\frac{\cos\theta}{\sin\theta} \frac{\partial_\theta g}{g} + \frac{\partial_\theta^2 g}{g} + \left(\frac{1}{\tan^2\theta} - \frac{\omega_{(0)}^2}{\omega^2} \right) \frac{\partial_\varphi^2 f}{f} \right] &(141)
\end{aligned}$$

Our separation of variables is complete and we immediately realize that $\frac{\partial_\varphi^2 f}{f}$ must be constant. The homogeneous differential equation for φ is

$$\frac{\partial_\varphi^2 f}{f} = -m^2 \tag{142}$$

with $m = 0, 1, 2, ...$ and solved by

$$f(\varphi) = e^{im\varphi} \tag{143}$$

We can use this result and now have a differential equation dependent only on the variable θ:

$$\frac{1}{f}\Box_x(fg) = \Box_x g \tag{144}$$

$$= \omega^2 \left[\frac{\cos\theta}{\sin\theta}\frac{\partial_\theta g}{g} + \frac{\partial_\theta^2 g}{g} + \left(\frac{1}{\tan^2\theta} - \frac{\omega_{(0)}^2}{\omega^2} \right)(-m^2) \right] \tag{145}$$

$$= \omega^2 \left[\frac{\cos\theta}{\sin\theta}\frac{\partial_\theta g}{g} + \frac{\partial_\theta^2 g}{g} + m^2 \left(\frac{\omega_{(0)}^2}{\omega^2} - \frac{1}{\tan^2\theta} \right) \right] \tag{146}$$

This looks complicated so we go to what we know: The eigenvalue equation for spherical Laplacians can usually be solved by (associated) Legendre polynomials. We will remind ourselves how these look like [19] and will try to bring our equation to the appropriate form.

The associated Legendre polynomials $P_l^m(s)$ solve an ordinary differential equation of the form

$$\partial_s((1-s^2)\partial_s p) + \left(\gamma - \frac{m^2}{1-s^2} \right) p = \lambda p \tag{147}$$

where $p = p(s)$. The eigenvalues are $\gamma = l(l+1)$ where l is an integer $0 \leq m \leq l$ and the eigenfunctions are

$$P_l^m(s) = \frac{(-1)^m}{2^l l!}(1-s^2)^{m/2}\frac{d^{l+m}}{ds^{l+m}}[(s^2-1)^l] \tag{148}$$

these are the a bit more complicated version of the Legendre polynomials $P_l(s)$

$$P_l(s) = \frac{1}{2^l l!}\frac{d^l}{ds^l}(s^2-1)^l \qquad P_l(1) = 1 \tag{149}$$

in terms of these the associated Legendre functions are

$$P_l^m(s) = (1-s^2)^{m/2}\frac{d^m}{ds^m}P_l(s) \tag{150}$$

The associated Legendre differential equation is therefore solved by

$$\partial_s((1-s^2)\partial_s P_l^m(s)) + \left(\gamma - \frac{m^2}{1-s^2} \right) P_l^m(s) = l(l+1)P_l^m(s) \tag{151}$$

where m, l are integers and $m = -l, ..., +l$.

Let $s = \cos\theta$ so that $\sin^2\theta = 1 - \cos^2\theta = 1 - s^2$, then the differential equation takes the following form (compare e.g. [19])

$$\partial_\theta^2 p + \frac{\cos\theta}{\sin\theta}\partial_\theta p + \left[\gamma - \frac{m^2}{\sin^2\theta}\right] p = \lambda p \tag{152}$$

Now that we've refreshed our memory we can compare our differential equation Eq. (146) with Eq. (152) by rewriting it as follows:

$$\frac{1}{f}\Box_x(fg) = \Box_x g = \omega^2 \left[\partial_\theta^2 + \frac{\cos\theta}{\sin\theta}\partial_\theta + m^2\left(\frac{\omega_{(0)}^2}{\omega^2} - \frac{1}{\tan^2\theta}\right)\right] g \tag{153}$$

$$= \omega^2 \left[\partial_\theta^2 + \frac{\cos\theta}{\sin\theta}\partial_\theta + m^2\left(\frac{\omega_{(0)}^2}{\omega^2} - \frac{1-\sin^2\theta}{\sin^2\theta}\right)\right] g \tag{154}$$

$$= \omega^2 \left[\partial_\theta^2 + \frac{\cos\theta}{\sin\theta}\partial_\theta + m^2\left(\frac{\omega_{(0)}^2}{\omega^2} - \left(\frac{1}{\sin^2\theta} - 1\right)\right)\right] g \tag{155}$$

$$= \omega^2 \left[\partial_\theta^2 + \frac{\cos\theta}{\sin\theta}\partial_\theta + \left(m^2\left(\frac{\omega_{(0)}^2}{\omega^2} + 1\right) - \frac{m^2}{\sin^2\theta}\right)\right] g \tag{156}$$

This is already what we want! We see that our eigenvalue equation

$$\Box_x\phi = \Lambda\phi \tag{157}$$

in terms of spherical coordinates

$$\omega^2\Box_g\phi - \left(1 + \frac{\omega^2}{\omega_{(0)}^2}\right)\omega_{(0)}^2\partial_\varphi^2\phi = \Lambda\phi \tag{158}$$

can be rewritten as

$$\frac{1}{f}\Box_x(fg) = \Box_x g = \omega^2 \left[\partial_\theta^2 + \frac{\cos\theta}{\sin\theta}\partial_\theta + \left(m^2\left(\frac{\omega_{(0)}^2}{\omega^2} + 1\right) - \frac{m^2}{\sin^2\theta}\right)\right] g \tag{159}$$

and compared to Eq. (152). We identify

$$\omega^2 m^2\left(\frac{\omega_{(0)}^2}{\omega^2} + 1\right) = \omega^2\gamma = \omega^2 l(l+1) \tag{160}$$

from the associated Legendre equation and therefore see that $\Box_x\phi = \Lambda\phi$ is solved by the eigenvalues

$$\Lambda = \omega^2 l(l+1) - \left(\omega_{(0)}^2 + \omega^2\right) m^2 \tag{161}$$

with the eigenfunctions such that

$$\Box_x P_l^m(\cos\theta)e^{im\varphi} = \Lambda P_l^m(\cos\theta)e^{im\varphi} \tag{162}$$

but this is, up to a relatively arbitrary normalization condition, exactly the definition of the spherical harmonics that we've encountered before!

$$Y_{l,m}(\theta,\varphi) = NP_l^m(\cos\theta)e^{im\varphi} \tag{163}$$

with

$$Y^*_{l,m}(\theta,\varphi) = (-1)^m Y_{l,-m}(\theta,\varphi) \tag{164}$$

This means that we have seen for the second time that the differential equation for the deformed fuzzy sphere Laplacian $\Box_x$ is solved by the *fuzzy* spherical harmonics (these have a cutoff at $l = N$)

$$\Box_x \bar{Y}_{lm} = \left(\omega^2 l(l+1) - \left(\omega^2_{(0)} + \omega^2\right) m^2\right) \bar{Y}_{lm} \tag{165}$$

and can be comfortable using this result.

3.4 Symplectic form

The biggest chunk of legwork is done now. But to complete our analysis of this system we still need to be able to do integration. For this we look at the symplectic structure.

In math terms, the symplectic structure on the coadjoint orbit of a Lie Algebra is defined by a Poisson bracket and symplectic 2-form Ω [7]

$$\Omega := \frac{1}{2}\Omega_{\mu\nu} dx^\mu \wedge dx^\nu \tag{166}$$

the symbol $\wedge$ is called a *wedge product* or *exterior product* and is an antisymmetric product of differential forms.

Ω defines the basic geometric structure of the phase space and transforms as a covariant rank-two tensor. It is closed and non-degenerate. Ω is antisymmetric just like the Poisson brackets and also non-degenerate and closed. The closure, in local coordinates, is the same as the statement $\partial_\mu \Omega_{\alpha\nu} + \partial_\nu \Omega_{\mu\alpha} + \partial_\alpha \Omega_{\nu\mu} = 0$. This corresponds to the Jacobi identity for the Poisson brackets. The relationship between the symplectic form and the Poisson brackets is as follows:

$$\{f, g\} = \Omega^{\mu\nu} \partial_\mu f \partial_\nu g \tag{167}$$

If you recall, we have already done most of the required calculation for spherical coordinates when we were looking for the Poisson brackets in terms of the variables φ, θ. Note that we used y_μ as the spherical coordinates, but our semi-classical coordinates x_μ have but a linear relationship with y_μ which allows the use of the spherical coordinate Poisson bracket here.

We reiterate what we've found before in Eq. (113):

$$\{f(\varphi), g(\theta)\} = \frac{\partial f}{\partial \varphi}\frac{\partial g}{\partial \theta}\{\varphi, \theta\} \tag{168}$$

$$\Rightarrow \{\varphi, \theta\} = -(r\sin\theta)^{-1} \tag{169}$$

[7] you will often see the variable ω instead of Ω but the small omega is already occupied as a variable.

where the functions where chosen such that $f(\varphi) = \tan\varphi, g(\theta) = r\cos\theta$.

We can immediately read off the contravariant symplectic 2-form:

$$\Omega^{\mu\nu}(\varphi,\theta) = \begin{pmatrix} 0 & (r\sin\theta)^{-1} \\ -(r\sin\theta)^{-1} & 0 \end{pmatrix} \tag{170}$$

We also know that

$$\Omega^{\mu\nu}\Omega_{\nu\rho} = \delta^{\mu}_{\rho} \tag{171}$$

so the inverse is easily calculated:

$$\Omega_{\mu\nu}(\varphi,\theta) = \begin{pmatrix} 0 & -r\sin\theta \\ r\sin\theta & 0 \end{pmatrix} \tag{172}$$

Thus,

$$\Omega := \frac{1}{2}\Omega_{\mu\nu}dx^{\mu} \wedge dx^{\nu} = r\sin\theta d\varphi \wedge d\theta \tag{173}$$

We now look at an important property of the symplectic form:

$$\int_{\mathcal{M}} \Omega = 2\pi n \tag{174}$$

where $n \in \mathbb{N}$ and $\mathcal{M}$ is a noncontractible two-surface like e.g. our spheroid. This is basically the same as requiring that wave functions on this space are single-valued. This is of course true when our $\mathcal{M}$ is the surface of a sphere or, respectively, a sphere that is slightly deformed. [20][18]

This is often called a quantization condition. That's because given a quantization map $\mathcal{Q}$ which transports a function f to a quantized version of it, $\mathcal{Q}(f)$, we have as a property of the trace

$$\mathrm{Tr}\left(\mathcal{Q}(f)\right) = \frac{1}{2\pi}\int_{S^2} \Omega f \tag{175}$$

so this is why we needed to find the symplectic form.

3.5 Quantization Map and Important Results

We can take all of the results obtained in this chapter to form our quantization map. Let us first reiterate the definition of a quantization map:

Definition: Let $\mathcal{M}$ be a Poisson manifold. A linear map

$$\mathcal{Q} : \mathcal{C}(\mathcal{M}) \to \mathrm{End}(\mathcal{M}) \tag{176}$$

satisfying the axioms

- $\mathcal{Q}(1) = \mathbb{I}$
- $\mathcal{Q}(f)^{\dagger} = \mathcal{Q}(f^{*}) \quad \forall f \in \mathcal{C}(\mathcal{M})$
- *the correspondence principle:* (κ is the scale / quantization parameter)
  $\lim\limits_{\kappa\to 0} \frac{1}{\kappa}\left([\mathcal{Q}(f), \mathcal{Q}(g)] - i\mathcal{Q}\left(\{f,g\}\right)\right) = 0 \quad \forall f,g \in \mathcal{C}(\mathcal{M})$
  $\lim\limits_{\kappa\to 0}\left(\mathcal{Q}(fg) - \mathcal{Q}(f)\mathcal{Q}(g)\right) = 0 \;\; \forall f,g \in \mathcal{C}(\mathcal{M})$

- *irreducibility:*
  If $\{f_i, g\} = 0 \quad \forall i \in I$ implies $g \propto 1$
  then $[\mathcal{Q}(f_i), A] = 0 \quad \forall i \in I$ implies $A \propto 1$

is called a quantization map.

The quantization map for the fuzzy sphere considered here is the following:

$$\mathcal{Q} : \mathcal{C}(S^2) \to Mat(N, \mathbb{C}) \tag{177}$$

$$x^\mu \mapsto X^\mu = \omega_{(\mu)} J^\mu \tag{178}$$

$$Y^l_m \mapsto \begin{cases} \bar{Y}^l_m & l < N \\ 0 & l \geq N \end{cases} \tag{179}$$

J^a are the generators of $su(2)$ in the N-dimensional irreducible representation. The $\bar{Y}^l_m$ are the so-called fuzzy spherical harmonics with a cut-off at $l = N$.

The generators X^μ of the algebra $Mat(N, \mathbb{C})$ satisfy the commutation relations

$$\boxed{[X_\mu, X_\nu] = i\epsilon_{\mu\nu\rho} \frac{\omega_{(\mu)}\omega_{(\nu)}}{\omega_{(\rho)}} X_\rho} \tag{180}$$

where $\mu = 0, 1, 2$.

The X^μ are the generators of this fuzzy sphere and a quantization of functions x^μ in the Euclidean space $\mathbb{R}^3$:

$$X^\mu = \mathcal{Q}(x^\mu) : \quad S^2 \hookrightarrow \mathbb{R}^3 \tag{181}$$

We see that the algebra $Mat(N, \mathbb{C})$ can be decomposed into irreducible representations under the adjoint action of $su(2)$:

$$Mat(N, \mathbb{C}) \approxeq \mathbb{C}^N \otimes \mathbb{C}^N \tag{182}$$

$$= (1) \oplus (3) \oplus \cdots \oplus (2N-1) \tag{183}$$

$$= \{\bar{Y}^0_0\} \oplus \cdots \oplus \{\bar{Y}^N_m\} \tag{184}$$

where $\bar{Y}$ are precisely the fuzzy spherical harmonics mentioned above. They satisfy the orthonormalization condition:

$$\int_{S^2} \frac{d\Omega}{4\pi} \bar{Y}^*_{lm}(\theta, \varphi) \bar{Y}_{l'm'}(\theta, \varphi) = \delta_{ll'}\delta_{mm'} \tag{185}$$

The Laplacian on this fuzzy sphere has a correction term to the Laplacian on the usual fuzzy sphere:

$$\boxed{\Box_x \phi = \omega^2 C^{(2)} \phi - \left(1 + \frac{\omega^2}{\omega^2_{(0)}}\right) \{x_0, \{x_0, \phi\}\}} \tag{186}$$

which for spherical coordinates reads:

$$\boxed{\Box_x \phi = \omega^2 C^{(2)} \phi - \left(1 + \frac{\omega^2}{\omega^2_{(0)}}\right) \partial^2_\varphi \phi} \tag{187}$$

We also found that the eigenvalue equation for the modified box operator

$$\Box_x \phi = \Lambda \phi \tag{188}$$

is solved by the fuzzy spherical harmonics

$$\Box_x \bar{Y}_{lm} = \left(\omega^2 l(l+1) - \left(\omega_{(0)}^2 + \omega^2\right) m^2\right) \bar{Y}_{lm} \tag{189}$$

with $l = 0, 1, 2, ..., N-1$, $m = -l, ..., +l$

At last we recall the symplectic form on the sphere:

$$\Omega := \frac{1}{2} \Omega_{\mu\nu} dx^\mu \wedge dx^\nu = r \sin\theta d\varphi \wedge d\theta \tag{190}$$

4 Scalar Fields on my Fuzzy Sphere

We began our adventure with this action:

$$S(X) = \frac{1}{g}\,\mathrm{Tr}\left(\frac{1}{4}\eta_{\mu\mu'}\eta_{\nu\nu'}[X^{\mu'},X^{\nu'}][X^{\mu},X^{\nu}] - \frac{\mu^2}{2}X_iX^i + \frac{\mu_0^2}{2}X_0X^0\right) \tag{191}$$

We now want to look at this acting on a scalar function ϕ.

4.1 An educational failure

First, we will try to do this by using the following action for a real scalar function:

$$S(\phi) = \frac{1}{g}\,\mathrm{Tr}\left(\frac{1}{4}\eta_{\mu\nu}[X^{\mu},\phi][X^{\nu},\phi] + \frac{m_\phi^2}{2}|\phi|^2\right) \tag{192}$$

where $m_\phi^2 \in \mathbb{R}$. However, we will soon see that we cannot find any on-shell solutions. It is educational to see how that happens.

First recall some useful properties of the trace:

$$\mathrm{Tr}\left([X,f][X,f]\right) = \mathrm{Tr}\left(f[X,[X,f]]\right) \qquad\qquad \mathrm{Tr}\left(\mathcal{Q}(f)\right) = \frac{1}{2\pi}\int_{S^2}\Omega f \tag{193}$$

From this we see that we can rewrite the action in terms of semi-classical coordinates by replacing the commutators with our special Laplacian and the trace by an integral with respect to the symplectic form. Note that the Laplacian has the correction term as shown above (94). The action now reads:

$$S(\phi) = \frac{1}{g}\int_{S^2}\left(\frac{1}{4}\phi\Box_x\phi + \frac{m_\phi^2}{2}|\phi|^2\right) \tag{194}$$

Reminder: The eigenvalue-equation $\Box_x\phi = \Lambda\phi$ was solved by fuzzy spherical harmonics with the eigenvalues $\Lambda = \omega^2 l(l+1) - \left(\omega_{(0)}^2 + \omega^2\right)m^2$, where $l = 0,1,2,...,N-1$, $m = -l,...,+l$.

Therefore, it is best to decompose the scalar function in terms of the fuzzy spherical harmonics [8] into

$$\phi(\theta,\varphi) = \sum_{l=0}^{N-1}\sum_{m=-l}^{+l}\phi_{lm}Y_{lm}(\theta,\varphi) \tag{195}$$

$$\phi_{lm} = \int_{S^2}\frac{d\Omega}{4\pi}Y_{lm}^*(\theta,\varphi)\phi(\theta,\varphi) \tag{196}$$

with the orthonormalization condition

$$\int_{S^2}\frac{d\Omega}{4\pi}Y_{lm}^*(\theta,\varphi)Y_{l'm'}(\theta,\varphi) = \delta_{ll'}\delta_{mm'} \tag{197}$$

With this decomposition the action can be written as

[8] we ommit the bar on top of the spherical harmonics which indicated that they have a cutoff until now; all spherical harmonics in this chapter are fuzzy and cut off at $l = N$.

$$S(\phi) = \frac{1}{g}\sum_{l=0}^{N-1}\sum_{m=-l}^{+l}\frac{1}{4}\left(\omega^2 l(l+1) - (\omega_{(0)}^2 + \omega^2)m^2 \ + 2m_\phi^2\right)\phi_{lm}^2 \tag{198}$$

If we now look at the Euler-Lagrange equations

$$\partial_\mu \frac{\partial L}{\partial(\partial_\mu \phi)} - \frac{\partial L}{\partial \phi} = 0 \tag{199}$$

where we use the decomposed form of the action and therefore simplify $L = L(\phi_{lm})$ to:

$$L(\phi_{lm}) = \frac{1}{4}\left(\omega^2 l(l+1) - (\omega_{(0)}^2 + \omega^2)m^2 + 2m_\phi^2\right)\phi_{lm}^2 \tag{200}$$

then we see at once that the equations of motion would read:

$$\left(\omega^2 l(l+1) - (\omega_{(0)}^2 + \omega^2)m^2 + 2m_\phi^2\right)\phi_{lm} = 0 \tag{201}$$

but these would be discrete as both l and m are integers.

This obstacle is not unique to this particular fuzzy sphere, but it has been useful to see how it happened.

4.2 Complex scalar field with Feynman prescription

We've seen that carrying the action over to semi-classical in a straightforward way does not give us what we've hoped for: We do not find on-shell solutions.

We therefore look at a complex scalar field and compute the scalar field propagator. The properties of the trace are obviously still the same, so we immediately look at the action in the following form:

$$S_\epsilon[\phi, \phi^*] = \frac{1}{g}\int_{\mathcal{M}} \Omega\ \phi^* \left(\Box_x + m_\phi^2 - i\epsilon\right)\phi \tag{202}$$

Recall that we found that the integral over our symplectic form is (Eq. 174):

$$\int_{\mathcal{M}} \Omega = 2\pi n \tag{203}$$

where we choose to let the constant g in our action swallow the n and all amounts of π's that will appear in the integration process. These would cancel anyway, so we can stop thinking about them right away.

We can now realize that

$$S_\epsilon[\phi,\phi^*] = \frac{1}{g}\int_{\mathcal{M}} \Omega\phi^* \left(\Box_x + m_\phi^2 - i\epsilon\right)\phi \tag{204}$$

$$= \frac{1}{g}\int_{\mathcal{M}} \Omega \left(\frac{1}{4}\phi^*\Box_x\phi + \frac{1}{2}(m_\phi^2 - i\epsilon)|\phi|^2\right) \tag{205}$$

$$= \frac{1}{g}\int_{\mathcal{M}} \Omega \;\; \frac{1}{4}\sum_{l,l'}\sum_{m,m'} \left(\omega^2 l(l+1) - \left(\omega_{(0)}^2 + \omega^2\right) m^2\right) Y_{lm}^*(\theta,\varphi)Y_{l'm'}(\theta,\varphi)\phi_{lm}^*\phi_{l'm'} \tag{206}$$

$$+ \frac{1}{2}\sum_{l,l'}\sum_{m,m'}(m_\phi^2 - i\epsilon)Y_{lm}^*(\theta,\varphi)Y_{l'm'}(\theta,\varphi)\phi_{lm}^*\phi_{l'm'} \tag{207}$$

$$= \sum_{l,m}\left(\omega^2 l(l+1) - (\omega_{(0)}^2 + \omega^2)m^2 + 2(m_\phi^2 - i\epsilon)\right)|\phi_{lm}|^2 \tag{208}$$

where in the second to last line we performed the integral using the orthonormalization condition of the spherical harmonics.

4.3 Two-point function

After finding a useful version of the action we can now move on to find the two-point function of the theory. It is given by

$$\langle\phi_{lm}\;\phi_{l'm'}\rangle = \frac{1}{Z}\int D\phi\;\phi_{lm}\;\phi_{l'm'}\;e^{iS_\epsilon[\phi]} \tag{209}$$

$$= \frac{1}{Z}\int D\phi\;\phi_{lm}\;\phi_{l'm'}e^{i\frac{1}{g}\int\Omega\;\phi^*\left(\Box_x + m_\phi^2 - i\epsilon\right)\phi} \tag{210}$$

where

$$Z = \int D\phi\;e^{iS_\epsilon[\phi]} \qquad\qquad D\phi = \prod d\phi_{lm} \tag{211}$$

Z is the zero-point function and we will have a look at it first.

Because our action is quite long we will define

$$W(l,m) := \left(\omega^2 l(l+1) - (\omega_{(0)}^2 + \omega^2)m^2 + 2(m_\phi^2 - i\epsilon)\right) \tag{212}$$

such that our action is more readable:

$$S_\epsilon[\phi,\phi^*] = \sum_{l,m}\left(\omega^2 l(l+1) - (\omega_{(0)}^2 + \omega^2)m^2 + 2(m_\phi^2 - i\epsilon)\right)\phi_{lm}^*\phi_{lm} \tag{213}$$

$$= \sum_{l,m} W(l,m)\phi_{lm}^*\phi_{lm} \tag{214}$$

We now plug it into the zero-point function Z

$$Z = \int D\phi\;\exp\left(\sum_{l,m} W(l,m)\phi_{lm}^*\phi_{lm}\right) \tag{215}$$

$$\tag{216}$$

This is a Gaussian integral, which means we must take a short detour to see how these can be solved in this case.

4.3.1 Complex Gaussian integral for matrices

In general the Gaussian integral for an N-dim positive definite Hermitian complex matrix B and an N-dimensional complex vector v is written as

$$\int d^{2N}v \exp\left(-\sum_{i,j=1}^{N} v_i^* B_{ij} v_j\right) = \int d^{2N}v e^{-v^\dagger B v} = \pi^N \det B^{-1} \tag{217}$$

where $d^{2N}v = \prod_{i=1}^{N} d\Re(v_i) d\Im(v_i)$.

We introduce a unitary matrix U which diagonalizes the matrix B:

$$U^\dagger B U = \mathrm{diag}(b_1, ..., b_N) \tag{218}$$

and introduce complex variables z:

$$z = U^\dagger v \Longleftrightarrow v = Uz \tag{219}$$

which we can use to find

$$v^\dagger B v = z^\dagger U^\dagger B U z = \sum_{i=1}^{N} b_i |z_i|^2 \tag{220}$$

we put this into the Gaussian integral to find the result:

$$\int d^{2N}v \exp\left(-\sum_{i,j=1}^{N} v_i^* B_{ij} v_j\right) = \int d^{2N}v e^{-v^\dagger B v} \tag{221}$$

$$= \int d^{2N}z \exp\left(-\sum_{i=1}^{N} b_i |z_i|^2\right) = \prod_{i=1}^{N} \frac{\pi}{b_i} = \frac{\pi^N}{\prod_{i=1}^{N} b_i} \tag{222}$$

$$= \frac{\pi^N}{\det B} \tag{223}$$

You might notice that usually there is a square-root in the solution of Gaussian integrals, however, we have twice as many variables here (real and imaginary).

This is the solution that we need for Z, the denominator of the two-point function. For the more complicated Gaussian integral we introduce a linear term into the exponent. Then the Gaussian integral becomes

$$\int d^{2N}v \ \exp\left(-v^\dagger B v + z^\dagger v + v^\dagger z\right) \tag{224}$$

We now complete the square:

$$- Bv^\dagger v + z^\dagger v + v^\dagger z \tag{225}$$

$$= -(v - B^{-1}z)^\dagger \ B \ (v - B^{-1}z) + z^\dagger B^{-1} z \tag{226}$$

we put this in and shift the integration variables:

$$\int d^{2N}v \ \exp\left(-v^\dagger Bv + z^\dagger v + v^\dagger z\right) \tag{227}$$

$$= \exp[z^\dagger B^{-1} z] \int d^{2N}v \ \exp\left[-(v - B^{-1}z)^\dagger \ B \ (v - B^{-1}z)\right] \tag{228}$$

$$= \exp[z^\dagger B^{-1} z] \int d^{2N}v \ \exp\left(-v^\dagger Bv\right) \tag{229}$$

$$= \exp[z^\dagger B^{-1} z] \frac{\pi^N}{\det B} \tag{230}$$

Similarly to the way we usually solve these integrals we will make use of the derivation properties of the exponential function to find solutions to more integrals.

$$\int d^{2N}v \ v^\dagger v \exp\left(-v^\dagger Bv + z^\dagger v + v^\dagger z\right) \tag{231}$$

$$= \partial_{z^\dagger}\partial_z \int d^{2N}v \ \exp\left(-v^\dagger Bv + z^\dagger v + v^\dagger z\right) \tag{232}$$

$$= \partial_{z^\dagger}\partial_z \left(e^{z^\dagger B^{-1} z} \frac{\pi^N}{\det B}\right) \tag{233}$$

$$= \frac{\pi^N}{\det B} \partial_{z^\dagger}\partial_z \left(e^{z^\dagger B^{-1} z}\right) \tag{234}$$

$$= \frac{\pi^N}{\det B} \partial_{z^\dagger} \left(z^\dagger B^{-1} e^{z^\dagger B^{-1} z}\right) \tag{235}$$

$$= \frac{\pi^N}{\det B} (\left((\partial_{z^\dagger} z^\dagger B^{-1}) e^{z^\dagger B^{-1} z} + z^\dagger B^{-1} (\partial_{z^\dagger} e^{z^\dagger B^{-1} z})\right) \tag{236}$$

$$= \frac{\pi^N}{\det B} \left(B^{-1} e^{z^\dagger B^{-1} z} + z^\dagger B^{-1} B^{-1} z e^{z^\dagger B^{-1} z}\right) \tag{237}$$

$$\tag{238}$$

We now set $z = 0$:

$$\int d^{2N}v \ v^\dagger v \exp\left(-v^\dagger Bv\right) \tag{239}$$

$$= \frac{\pi^N}{\det B} \left(B^{-1}\right) \tag{240}$$

$$\tag{241}$$

We now take the fraction of both integrals:

$$\frac{\int d^{2N}v \ v^\dagger v \exp\left(-v^\dagger Bv\right)}{\int d^{2N}v \ \exp\left(-v^\dagger Bv\right)} \tag{242}$$

$$= \frac{\frac{\pi^N}{\det B}\left(B^{-1}\right)}{\frac{\pi^N}{\det B}} \tag{243}$$

$$= B^{-1} \tag{244}$$

and have hereby completed our detour into Gaussian integrals. We can now find the two-point function:

$$\langle \phi_{lm} \ \phi_{l'm'} \rangle = \frac{\int D\phi \ \phi_{lm} \ \phi_{l'm'} \ e^{W(l,m)\phi^*\phi}}{\int D\phi \ \ e^{W(l,m)\phi^*\phi}} \tag{245}$$

$$= \delta_{ll'}\delta_{mm'} W(l,m)^{-1} \tag{246}$$

Remember that $W(l,m)$ was merely the replacement for a longer term to aid us during the calculation and we can plug it back in; the two-point function is then given by

$$\boxed{\langle\phi_{lm}\ \phi_{l'm'}\rangle = \Big(\omega^2 l(l+1) - (\omega_{(0)}^2 + \omega^2)m^2 + 2(m_\phi^2 - i\epsilon)\Big)^{-1}\delta_{ll'}\delta_{mm'}} \tag{247}$$

The scalar function in position space can be found by Fourier transform as follows:

$$\langle\phi(x)\ \phi(y)\rangle = \sum_{ll'mm'} Y_{lm}(x)Y^*_{l'm'}(y)\langle\phi_{lm}\ \phi_{l'm'}\rangle \tag{248}$$

$$= \sum_{ll'mm'} \frac{Y_{lm}(x)Y^*_{l'm'}(y)\delta_{ll'}\delta_{mm'}}{\omega^2 l(l+1) - (\omega_{(0)}^2 + \omega^2)m^2 + 2(m_\phi^2 - i\epsilon)} \tag{249}$$

$$= \sum_{lm} \frac{Y_{lm}(x)Y^*_{lm}(y)}{\omega^2 l(l+1) - (\omega_{(0)}^2 + \omega^2)m^2 + 2(m_\phi^2 - i\epsilon)} \tag{250}$$

and with this result we have almost everything we need to understand what happens on the modified fuzzy sphere. But before we go into the interpretation we will still have a look at the geometrical features in the next chapter.

5 Geometrical Considerations

To understand the properties of this fuzzy sphere better I will intersect here with a small study of the underlying geometric structure.

In general, the induced metric $h_{\mu\nu}(\xi)$ is the metric tensor defined on a submanifold Σ that is induced from the metric tensor $g_{\alpha\beta}(x)$on a manifold $\mathcal{M}$ into which the submanifold Σ is embedded.

$$h_{\mu\nu}(\xi) = g_{\alpha\beta}(x(\xi))\frac{\partial x^\alpha}{\partial \xi^\mu}(\xi)\frac{\partial x^\beta}{\partial \xi^\nu}(\xi) \tag{251}$$

where μ, ν are indices of coordinates ξ^a of the submanifold, while the functions $x^\mu(\xi^a)$ encode the embedding into the higher-dimensional manifold whose tangent indices are denoted α, β. [21]

For us, the metric tensor on the manifold $\mathcal{M}$ is just the Minkowski metric tensor $\eta_{\alpha\beta}$.

We know that $x^\mu = \omega_{(\mu)} y^\mu$, so in y-coordinates, the metric is

$$\boxed{ds_y^2(y) = -\omega_{(0)}^2 dy_0^2 + \omega^2(dy_1^2 + dy_2^2)} \tag{252}$$

which is clearly a Lorentzian metric.

But y^μ are also spherical coordinates, so we can write down explicitly:

$$x^\mu = \omega_{(\mu)} \begin{pmatrix} \cos\theta \\ \sin\theta\cos\varphi \\ \sin\theta\sin\varphi \end{pmatrix} \tag{253}$$

$$\partial_\theta x^\mu = \omega_{(\mu)} \begin{pmatrix} -\sin\theta \\ \cos\theta\cos\varphi \\ \cos\theta\sin\varphi \end{pmatrix} \tag{254}$$

$$\partial_\varphi x^\mu = \omega_{(\mu)} \begin{pmatrix} 0 \\ -\sin\theta\sin\varphi \\ \sin\theta\cos\varphi \end{pmatrix} \tag{255}$$

We see that the $h_{\theta\theta}$-component of the induced metric $h_{\mu\nu}$ (Eq. 251) does not agree with the usual metric on the sphere:

$$h_{\theta\theta} = (-\omega_{(0)}^2 \sin^2\theta + \omega^2\cos^2\theta)d\theta^2 \tag{256}$$

whereas $h_{\varphi\varphi}$ has (up to a constant) the usual value

$$h_{\varphi\varphi} = \omega^2 \sin^2\theta d\varphi^2 \tag{257}$$

The mixed components vanish.

Therefore, the induced metric ds_h^2 in spherical coordinates is

$$\boxed{ds_h^2(\theta,\varphi) = (-\omega_{(0)}^2 \sin^2\theta + \omega^2\cos^2\theta)d\theta^2 + \omega^2\sin^2\theta d\varphi^2} \tag{258}$$

For this metric to reduce to the usual spherical metric, we would need $\frac{\omega_{(0)}^2}{\omega^2} = -1$, which never happens since $\omega_{(0)}, \omega \in \mathbb{R}$.

We remind ourselves that we found $\omega_{(0)}^2 > \omega^2$ from the matrix equations of motion, Eq. (47), in the beginning of our journey and look at specific points for θ:

$$ds_h^2(0,\varphi) = ds_h^2(\pi,\varphi) = \omega^2 d\theta^2 \tag{259}$$

At the north and south pole (Eq. 259), where $\theta = 0, \pi$ respectively, $d\varphi^2$ becomes irrelevant as would be expected, and the metric is Euclidean.

$$ds_h^2(\frac{\pi}{2},\varphi) = -\omega_{(0)}^2 d\theta^2 + \omega^2 d\varphi^2 \tag{260}$$

Between $\theta = \pi/4$ and $\theta = 3\pi/4$ the metric is always Minkowski irrespective of the free parameters $\omega_{(0)}^2$ and ω^2.

For $\theta = \pi/2$ this is clear immediately (Eq. 260), for the rest of the interval we know this because $\omega_{(0)}^2 > \omega^2$ always, which makes the sign in Eq. (261) in front of $d\theta^2$ even for $\theta = \frac{\pi}{4}$ and $\theta = \frac{3\pi}{4}$ negative.

$$ds_h^2(\frac{\pi}{4},\varphi) = ds_h^2(\frac{3\pi}{4},\varphi) = -\frac{1}{2}(\omega_{(0)}^2 - \omega^2)d\theta^2 + \frac{1}{2}\omega^2 d\varphi^2 \tag{261}$$

From then on, the signature depends on the values of $\omega_{(0)}^2$ and ω^2. Let's look at that dependence:

$$(-\omega_{(0)}^2 \sin^2\theta + \omega^2 \cos^2\theta) = 0 \tag{262}$$

$$\Rightarrow \theta = \arctan\left(\sqrt{\frac{\omega_{(0)}^2}{\omega^2}}\right) \tag{263}$$

I've chosen not to evaluate the square root and keep $\sqrt{\frac{\omega^2}{\omega_{(0)}^2}}$ because since the time we've chosen $\omega_{(1)}^2 = \omega_{(2)}^2 = \omega^2$ in chapter 2 we have only dealt with the squares of ω and $\omega_{(0)}$.

The ratio $\frac{\omega^2}{\omega_{(0)}^2}$ must be between 0 and 1 (again, because $\omega_{(0)}^2 > \omega^2$).

From now on we will use the inverse of this ratio, $\frac{\omega_{(0)}^2}{\omega^2}$ to keep everything consistent with other results. This means that in the following plot the axis starts at the value $\frac{\omega_{(0)}^2}{\omega^2} = 1$. This switcheroo might seem confusing now but this way there is no confusion when comparing to all other upcoming plots in chapter 6.

Let's examine Fig. 1. This is a plot of Eq. 263 with a logarithmic horizontal axis. We can see where the signature changes with increasing value of $\frac{\omega_{(0)}^2}{\omega^2}$. The upper region of the plot above the curve is colored blue to indicate the negative signature (Minkowski) region. The lower region underneath the curve is colored green and represents the positive signature (Euclidean) region. As the ratio $\frac{\omega_{(0)}^2}{\omega^2}$ increases the region with Euclidean signature quickly shrinks to a small region around the poles. (It looks the same for the south and north pole). We also see dashed lines to indicate specific values of the ratio $\frac{\omega_{(0)}^2}{\omega^2}$; some of these will serve as examples in the following plot, Fig. 2, and we will look at these values even more closely in Chapter 6.

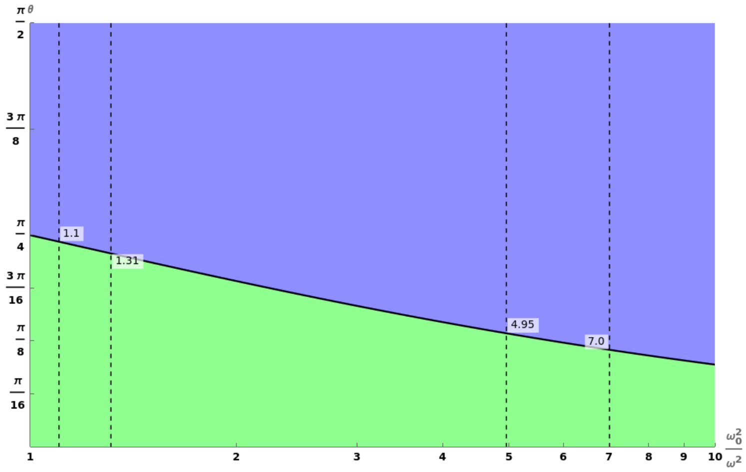

Figure 1: The signature change of the metric in the region $0 < \theta < \frac{\pi}{2}$ as it depends on the value of $\frac{\omega_{(0)}^2}{\omega^2}$. The horizontal axis is logarithmic. The values $\frac{\omega_{(0)}^2}{\omega^2} = (1.1, 1.31, 4.95, 7)$ are specifically marked. The Minkowski region is colored blue, the Euclidean region is colored green.

In Fig. 2 we see where the signature change on spheroids for some example values of $\frac{\omega_{(0)}^2}{\omega^2}$ takes place. In Fig. 2a where $\frac{\omega_{(0)}^2}{\omega^2} = 1.1$ the signature change happens close to $\frac{\pi}{4} = 45°$ and $\frac{3\pi}{4} = 135°$, specifically at $\theta = 43.6°$ and $\theta = 136.4°$. The next spheroid Fig. 2b with $\frac{\omega_{(0)}^2}{\omega^2} = 1.31$ is already visible elongated and has its signature changes already at $\theta = 41.1°$ and $\theta = 138.9°$. The third spheroid Fig. 2c with $\frac{\omega_{(0)}^2}{\omega^2} = 4.95$ is actually scaled to 33% to make it fit to the page. Here the green Euclidean region is already very small: The signature changes happen at $\theta = 24.2°$ and $\theta = 155.8°$. This is approximately at $\theta \approx \frac{\pi}{7}$ and $\theta \approx \frac{6\pi}{7}$.

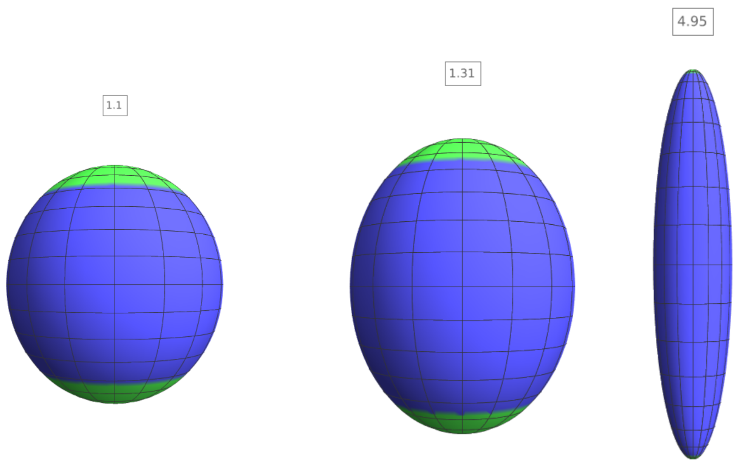

(a) $\frac{\omega_{(0)}^2}{\omega^2} = 1.1$

(b) $\frac{\omega_{(0)}^2}{\omega^2} = 1.31$

(c) $\frac{\omega_{(0)}^2}{\omega^2} = 4.95$

Figure 2: The signature change specifically on the spheroid with the values $\frac{\omega_{(0)}^2}{\omega^2} = (1.1, 1.31, 4.95)$. The spheroid in (c) with $\frac{\omega_{(0)}^2}{\omega^2} = 4.95$ is scaled to 33% of the size of the other spheroids.

The slope of the lightcones is easily found:

$$s_h^2(\theta,\varphi) = (-\omega_{(0)}^2 \sin^2\theta + \omega^2\cos^2\theta)d\theta^2 + \omega^2\sin^2\theta d\varphi^2 = 0 \tag{264}$$

$$d\varphi^2 = \frac{\omega_{(0)}^2 \sin^2\theta - \omega^2\cos^2\theta}{\omega^2\sin^2\theta} d\theta^2 \tag{265}$$

$$\frac{d\varphi}{d\theta} = \sqrt{\frac{\omega_{(0)}^2 \sin^2\theta - \omega^2\cos^2\theta}{\omega^2\sin^2\theta}} \tag{266}$$

The trajectory of the lightcones is given by:

$$s_h^2(\theta,\varphi) = (-\omega_{(0)}^2 \sin^2\theta + \omega^2\cos^2\theta)d\theta^2 + \omega^2\sin^2\theta d\varphi^2 = 0 \tag{267}$$

$$d\varphi^2 = \frac{\omega_{(0)}^2 \sin^2\theta - \omega^2\cos^2\theta}{\omega^2\sin^2\theta} d\theta^2 \tag{268}$$

$$\varphi = \int \sqrt{\left(\frac{\omega_{(0)}^2}{\omega^2} + 1 - \frac{1}{\sin^2\theta}\right)} d\theta \tag{269}$$

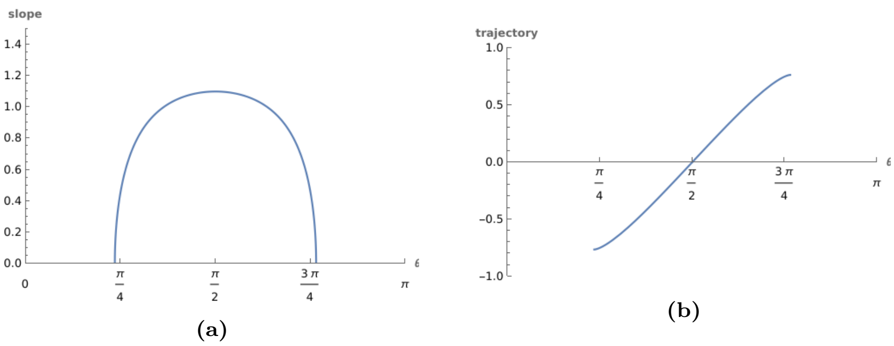

Figure 3: The slope (a) and the trajectory (b) of the lightcones for the spheroid with $\frac{\omega_{(0)}^2}{\omega^2} = 1.1$.

The slope and trajectory for the lightcone where $\frac{\omega_{(0)}^2}{\omega^2} = 1.1$ are shown in Fig. 3. We see that the lightcone begins close to $\theta \approx \pi/4$ and ends at approximately $\theta \approx 3\pi/4$ which is consistent with the information we've seen on the previous page.

6 Visualisation

In this section we will finally look at the results. Apart from the fact that they give a really pretty graphic resembling woven fabric and I will hang some on my wall they do tell us a lot about the equations we've seen here.

First, we will look at the results where I chose $\frac{\omega_{(0)}^2}{\omega^2} = 1.1$ (remember that $\omega_{(0)}^2 > \omega^2$ and therefore we will never see an exact sphere). We sit at the equator of the spheroid, as indicated by a red dot in Fig. 4a. This plot is generated via use of the formula for a spheroid

$$\frac{x_0^2}{\omega_{(0)}^2} + \frac{x_1^2}{\omega^2} + \frac{x_2^2}{\omega^2} = 1 \tag{270}$$

with $\omega_{(0)}^2 = 1.1, \omega^2 = 1$.

The plots next to it, Fig. 4b and Fig. 4c represent the two-point propagator in position space

$$\langle\phi(x)\ \phi(y)\rangle = \sum_{lm} \frac{Y_{lm}(x)Y^*_{lm}(y)}{\omega^2 l(l+1) - (\omega^2_{(0)} + \omega^2)m^2 + 2(m^2_\phi - i\epsilon)} \tag{271}$$

evaluated at the equator where $\theta = \pi/2$ and, arbitrarily chosen, $\varphi = \pi/4$. This means that the coordinate dependence for one of the spherical harmonics is fixed such that $y = y(\theta, \varphi) = y(\pi/2, \pi/4)$ and we let the plot run through the coordinates of the second spherical harmonic ($x = x(\theta, \varphi)$).

In Figures 4b and 4c we see the same plot viewed from different viewpoints. Fig. 4c shows the effect of the signature change beautifully: Between $\theta = 0$ and $\theta \approx \pi/4$ we see a flat region, which corresponds nicely with the green region around the south pole of the spheroid in Fig. 4a. This repeats around the north pole as we move from $\theta \approx 3\pi/4$ to $\theta = \pi$.

In between those flat regions we can see what happens in the region that is indicated with a blue color on the representation of the spheroid in Fig 4a. We can clearly see lightcones that wrap around the spheroid! The colors dark-blue to light-blue indicate what we see explicitly in Fig. 4b: as φ goes around the spheroid, the value of the propagator goes up and down. This can be attributed to the trajectory of the lightcones which we've seen in Fig. 3b.

The wobbles inside the Minkowskian region are sets of reflections of the lightcones; their nature can be seen better in upcoming graphics.

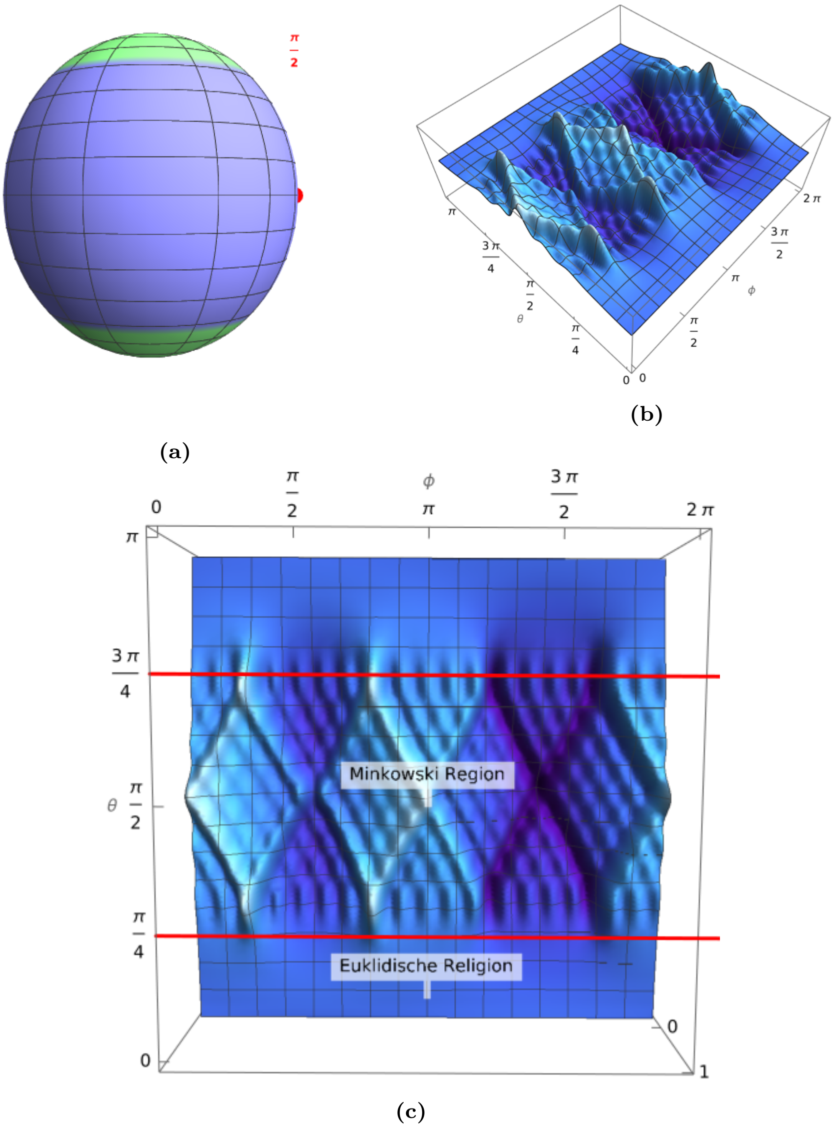

Figure 4: In (a) we see a representation of the spheroid with an indicator to tell us that we sit on the equator. (b) and (c) both show the evaluation of the scalar function as seen from this point. In (b) we see that the lightcones have different heights. (c) clearly shows where the signature changes.

Before we continue to explore what we see here, let us first compare these plots to the lightcones we would expect to see for a usual scalar field which doesn't live on a fuzzy sphere.

Fig. 5 are plots of the Feynman propagator $G_F(a, b)$ of a free scalar field with four-momentum p

$$G_F(a,b) = \lim_{\epsilon\to 0} \frac{1}{(2\pi)^4} \int d^4p \, \frac{e^{-ip(x-y)}}{(p^2 - m^2 \pm i\epsilon)} \tag{272}$$

$$= \begin{cases} -\frac{im}{4\pi^2}\delta(s) + \frac{mm}{8\pi 2\sqrt{s}} H_1^{(1)}(m\sqrt{s}) & s \geq 0 \\ -\frac{im}{4\pi^2\sqrt{-s}} K_1(m\sqrt{-s}) & s < 0 \end{cases} \tag{273}$$

$$s := (a^0 - b^0)^2 - (\vec{a} - \vec{b})^2 \tag{274}$$

where x, y are two points in Minkowski spacetime. $H_1^{(1)}$ is the Hankel function of the first kind and K_1 the modified Bessel function of the second kind. We choose $m = 1$ and show the absolute value as well as the real part and imaginary part separately.

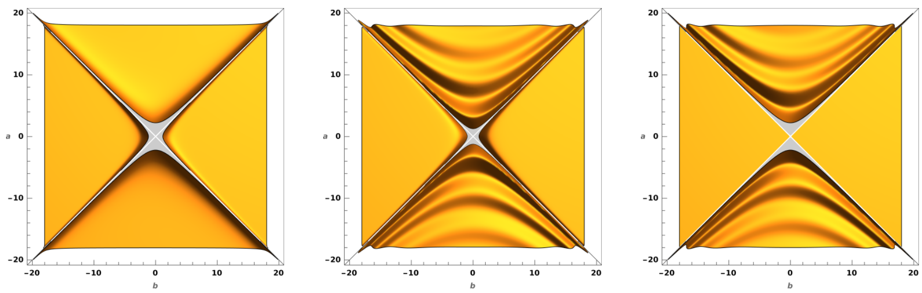

(a) **(b)** **(c)**

Figure 5: 3D plot of the free scalar field propagator $G_F(a,b)$. (a) shows the absolute value, (b) the real part and (c) the imaginary part.

We can see that the lightcone is clearly pronounced. If we were to extend the axes farther out the lightcone would simply continue on.

As we compare Fig. 5 to Fig. 4c we also notice that on the spheroid there are multiple lightcones as we move around the spheroid. There are actually only two distinct lightcones (one up, one down) which repeat with $\varphi = \pi$. I know this because these plots are evaluated where one of the spherical harmonics is fixed at $\theta = \pi/2, \varphi = \pi/4$ and the impression that the downward lightcone around $\varphi = \pi/4$ goes down less than the downward lightcone around $\varphi = 3\pi/4$ is an effect that stems from the position we've fixed the spherical harmonic in. The effect of the spherical harmonics can be seen more clearly in upcoming graphics (e.g., see Fig. 6c).

Let us now see what happens when we're not sitting directly on the equator but outside the Minkowskian region at $\frac{\pi}{8}$. Fig. 6a shows where we are on the spheroid. Next to it, in Fig. 6b we notice shadows of cones and a bright dot in the corner where $\theta = \pi/8, \varphi = \pi/4$. This dot appears precisely *because* we are in the positive-signature region: the spherical harmonics in the scalar field propagator dominate.

I've added another plot, Fig. 6c, that shows what the plain sum over the spherical harmonics at this point would look like:

$$\sum_{l=0}^{N} \sum_{m=-l}^{l} Y_{lm}(x) Y_{lm}^*(y) \qquad \text{with } \; y = y(\theta, \varphi) = (\frac{\pi}{8}, \frac{\pi}{4}) \tag{275}$$

We see immediately how this peak relates to the bright dot in Fig. 6b. Note that the wave pattern is only there because we cut off the spherical harmonics at $N = 30$. The spherical harmonics dominate only in the positive-signature region of the metric. Once we cross over to points in the negative-signature region of the metric, the peak becomes a lot less pronounced and the lightcones dominate the picture. However, we've seen that even at the equator there is the residual effect that the value of the propagator is slightly increased at $\varphi = \pi/4$, where we've fixed the value of one of the spherical harmonics.

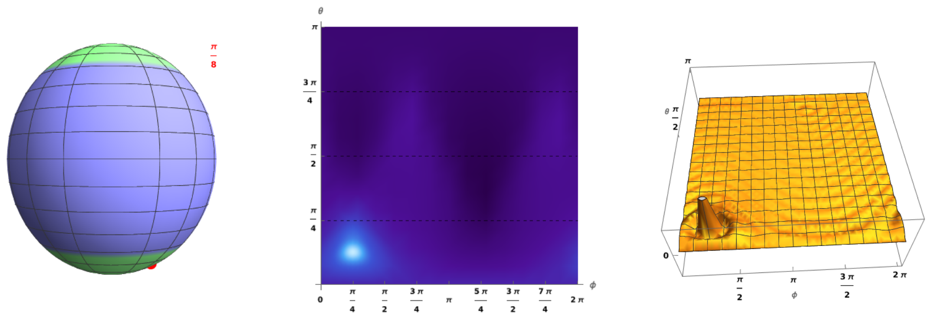

(a) (b) (c)

Figure 6: The flat region becomes smaller and smaller.

On the next page in Fig. 7 we see a whole set of plot-pairs for the spheroid with $\frac{\omega_{(0)}^2}{\omega^2} = 1.1$. We again see the spheroid with an indication of where we sit. Next to it is again the scalar field propagator evaluated at this point.

The first four pairs of plots are set at the values $\theta = \{\pi, \frac{15\pi}{16}, \frac{7\pi}{8}, \frac{13\pi}{16}\}$. These are all within the positive-signature region; we can see this also by the fact that the peak from the spherical harmonics is much brighter than the rest of the picture. It of course moves down the θ-axis from one plot to the next. The closer we get to the signature-change the better we start to see the shadow of lightcones.

Once we do cross over to the negative-signature region the fabric of the plots changes. We clearly see the flat region on the top and on the bottom as well as clear lightcones with the addition of a pattern of lightcone-reflections in the Minkowskian region. These are what I've called "wobbles" in our first encounter with them. They do not vanish when we look at larger sums (here $N = 30$) but are an intrinsic feature. We will return to this when we look at plots which carry less pronounced lightcones in Fig. 12.

At $\theta = \frac{3\pi}{4}$, very close to the signature change the lightcones only point toward the downward direction with a little bit of a frizz-like addition on the upper end that would be the beginning of cones toward the upward direction; these almost immediately end because they meet the signature change threshold and are cut off by the flat region. As we move down the spheroid with θ we can clearly see at what point on the spheroid we sit: At $\varphi = \frac{\pi}{4}$ and $\theta = \{\frac{3\pi}{4}, \frac{11\pi}{16}, \frac{5\pi}{8}, \frac{9\pi}{16}, \frac{\pi}{2}, \frac{3\pi}{8}, \frac{\pi}{4}\}$ the cones are crossing. Of course when $\theta = \frac{\pi}{2}$ they are equally long to both sides.

In the last three plot-pairs where $\theta = \{\frac{\pi}{8}, \frac{\pi}{16}, 0\}$ the spherical harmonics peak is again very visible, this time toward the bottom end of the plot according to the corresponding value of θ. Again the lightcones are but a shadow on these and become completely invisible on the pole.

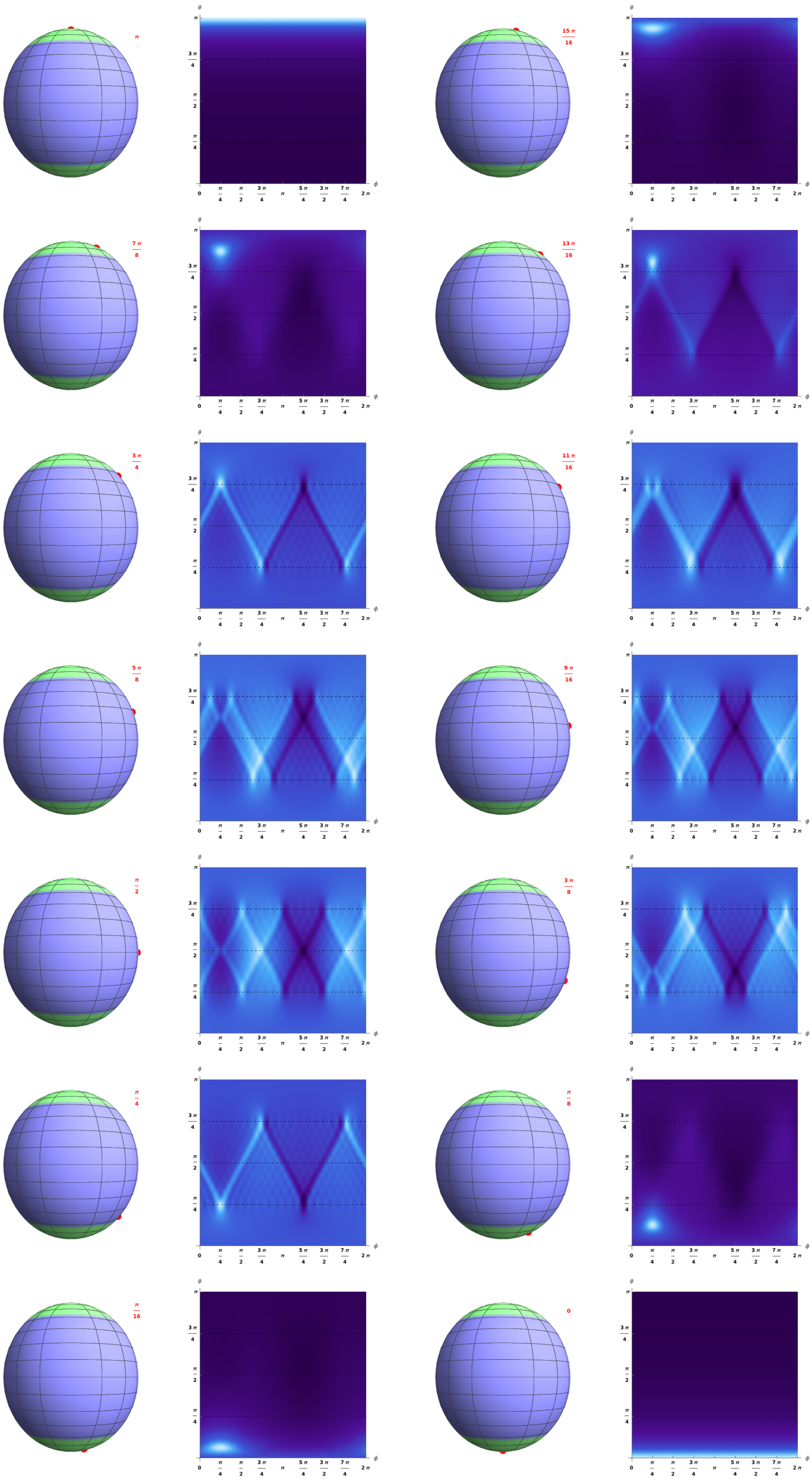

Figure 7: The metric as it looks from the perspective of different points on the sphere with a representation of the respective points on the spheroid. The ratio of $\frac{\omega_{(0)}^2}{\omega^2}$ here is 1.1

Next we want to see what happens when we change the ratio $\frac{\omega_{(0)}^2}{\omega^2}$. We've already seen in Fig. 2 that the spheroid elongates with an increasing ratio of $\frac{\omega_{(0)}^2}{\omega^2}$ and that the flat region becomes smaller. The set of plots on the next page, Fig. 8, gives us more information. Each row is dedicated to the same ratio $\frac{\omega_{(0)}^2}{\omega^2}$: In the first row $\frac{\omega_{(0)}^2}{\omega^2} = 1.1$, in the second $\frac{\omega_{(0)}^2}{\omega^2} = 1.31$, in the third $\frac{\omega_{(0)}^2}{\omega^2} = 4.95$ and in the fourth row $\frac{\omega_{(0)}^2}{\omega^2} = 7.0$. The lightcone-plots are all evaluated at the equator of the associated spheroid.

The first column gives us a taste of the shape of the spheroid we look at - note that I've scaled down the proportions of the spheroids for $\frac{\omega_{(0)}^2}{\omega^2} = \{4.95, 7.0\}$ such that they fit the page (they are about a fifth/tenth of their original size).

In the second column we see the lightcones proportional to the elongation of the associated spheroid: the θ-axis is stretched as compared to the φ-axis. We can see nicely how the flat region of the metric becomes smaller as the ratio $\frac{\omega_{(0)}^2}{\omega^2}$ increases. Additionally, it is clear from these proportionally adjusted plots that the angle between the cones stays the same irrespective of the ratio $\frac{\omega_{(0)}^2}{\omega^2}$.

However, if we imagine that we are tiny creatures sitting living on the spheroid our measurements would tell us that the lightcones look as they do in the third column. The lightcones are clearly stretched along the φ-axis and there are less lightcones as they wrap around the spheroid quicker. Instead, they repeat along the θ-axis until the flat region is reached. Conversely, as creatures living on such a spheroid we would be able to infer what type of spheroid we live on.

The following three pages show sets of plots analogous to Fig. 7 but for the ratios $\frac{\omega_{(0)}^2}{\omega^2} = \{1.31, 4.95, 7.0\}$. Again we move from the top of the spheroid where $\theta = \pi$ down toward the equator and further down toward $\theta = \frac{\pi}{16}$. From each plot to the next θ decreases by $\frac{\pi}{16}$. (Note to curious readers: In these I excluded the plot for $\theta = 0$ solely because then we would not have 4x4 plots per set; $\theta = 0$ looks the same for each spheroid because it's situated on the pole as is $\theta = \pi$.) Those sets of plots will be explained in more detail on the corresponding pages.

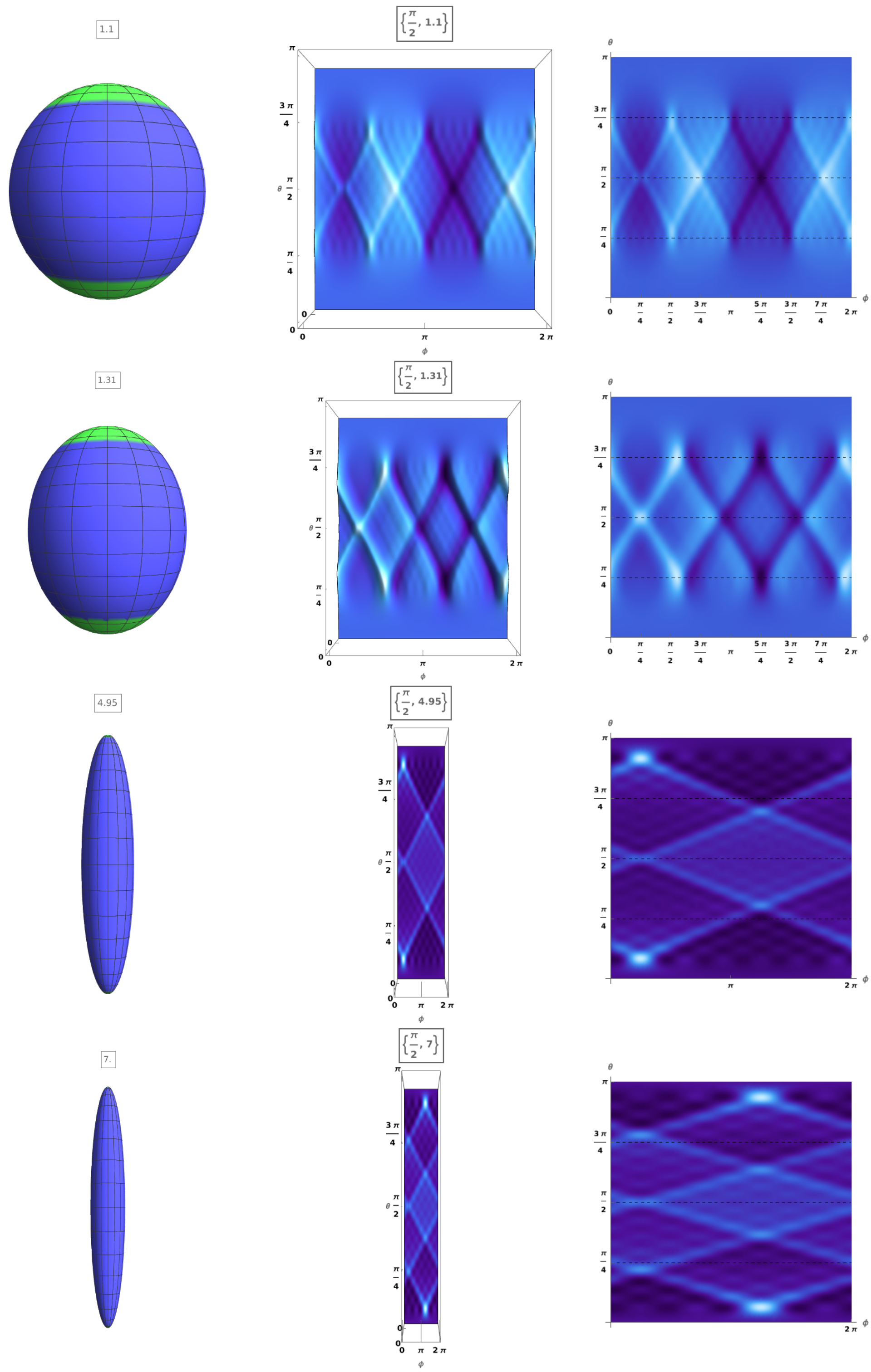

Figure 8: From top to bottom we see the same types of plots but with different values of the ratio $\frac{\omega_{(0)}^2}{\omega^2} = \{1.1, 1.31, 4.95, 7.0\}$. The first column shows the spheroid with the signature changes indicated: In the blue regions of the spheroids, the signature of the metric is negative, in the green region it is positive. In the second and third column we see the lightcones as seen from the equator. In the second column they are deformed (elongated φ-axis) according to the deformation of the sphere; the lightcones in the third column are at original axes values, this is what someone sitting on the equator would see.

Fig. 9 with $\frac{\omega_{(0)}^2}{\omega^2} = 1.31$ is still quite similar to the first set of plots we've seen. The flat region is confined to a smaller space. An additional feature is that we cross the threshold over to the negative-signature region sooner and the lightcones appear earlier.

For some plots, e.g. when $\theta = \{\frac{\pi}{4}, \frac{\pi}{2}\}$, there are very distinct lightcones as well. However, there are some points in between where there are multiple ones overlapping and although it is still conceivable to read off the fixed θ-value from the plots it is way less clear.

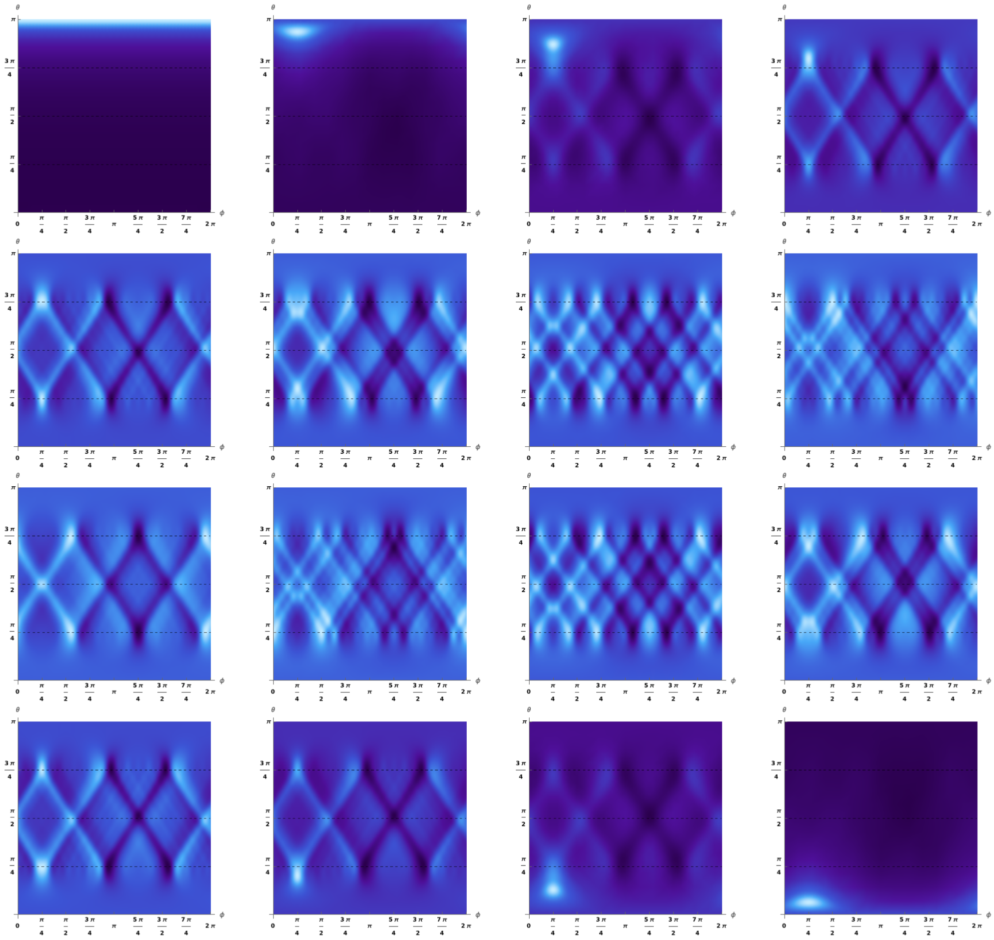

Figure 9: The metric as it looks from the perspective of different points on the spheroid. From the top left where $\theta = \pi$ to the bottom right where $\theta = \frac{\pi}{16}$ the fixed θ-value decreases in steps of $\frac{\pi}{16}$. In this set $\frac{\omega_{(0)}^2}{\omega^2} = 1.31$.

Fig. 10 with $\frac{\omega_{(0)}^2}{\omega^2} = 4.95$ is already quite different. Almost immediately after we move away from the pole we see the lightcone pattern. The one plot in the middle where there is a single distinct lightcone set sits at the equator; the others display quite beautiful superpositions. Interestingly, the plots toward the poles of the spheroid at $\theta = \{\frac{15\pi}{16}, \frac{\pi}{16}\}$show clearer lightcones again.

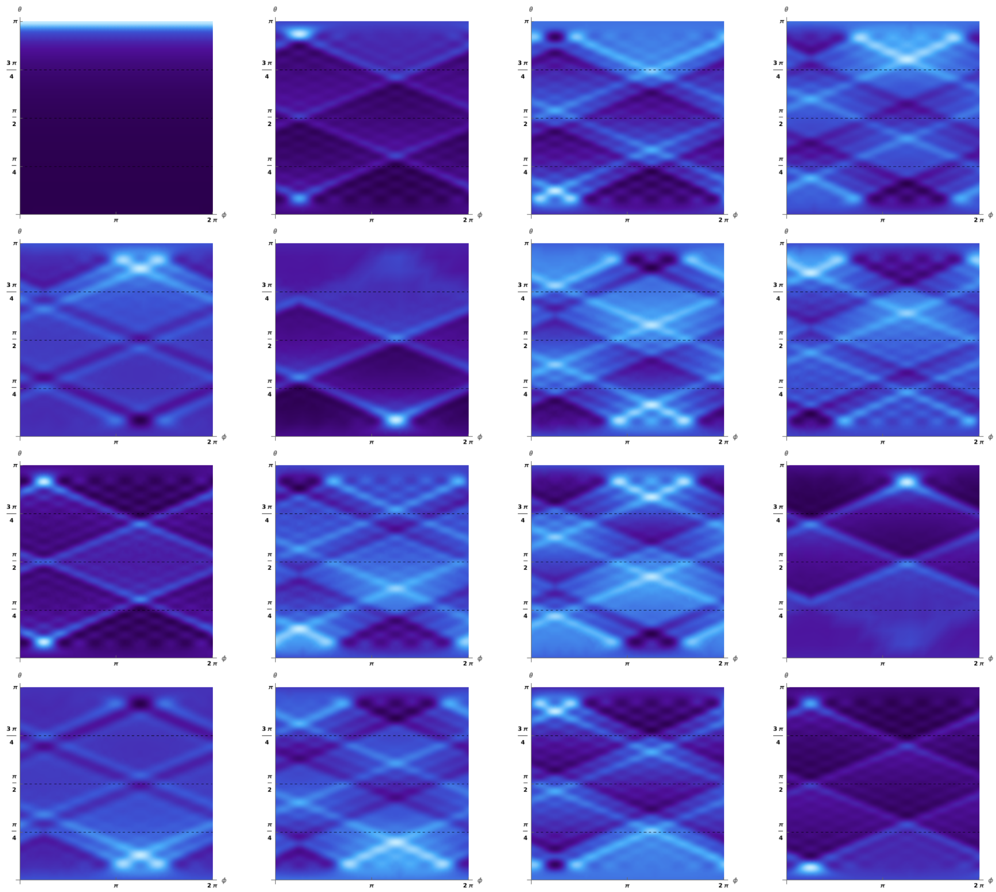

Figure 10: The metric as it looks from the perspective of different points on the spheroid. From the top left where $\theta = \pi$ to the bottom right where $\theta = \frac{\pi}{16}$ the fixed θ-value decreases in steps of $\frac{\pi}{16}$. In this set $\frac{\omega_{(0)}^2}{\omega^2} = 4.95$

Fig. 11 with $\frac{\omega_{(0)}^2}{\omega^2} = 7.0$ sees this trend continued with a lot of overlapping lightcones and even regions where they almost completely subtract from one another.

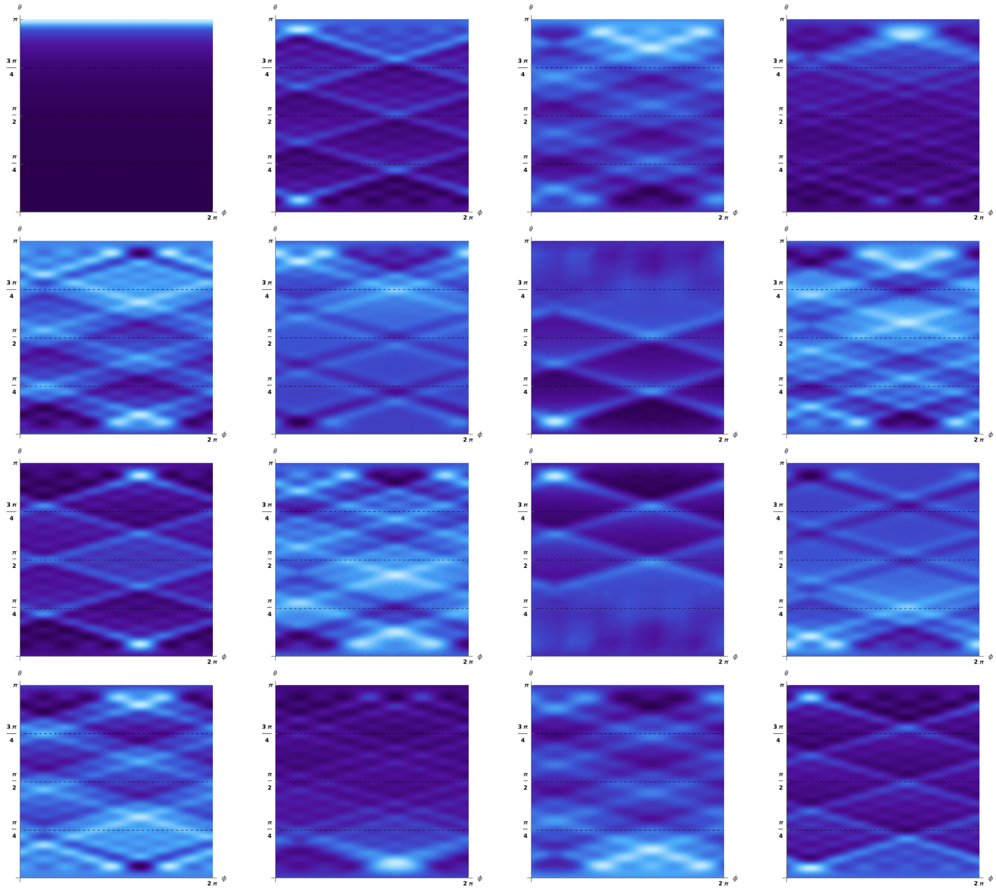

Figure 11: The metric as it looks from the perspective of different points on the spheroid. From the top left where $\theta = \pi$ to the bottom right where $\theta = \frac{\pi}{16}$ the fixed θ-value decreases in steps of $\frac{\pi}{16}$. In this set $\frac{\omega_{(0)}^2}{\omega^2} = 7.0$.

At last let me spend a moment on showing that we do not always see such marvelous lightcones. The ones we've seen above are where I've found the lightcones to be the most striking. In Fig. 12 we can see a set of plots of the scalar field propagator as seen from the equator of the respective spheroids – the ratio $\frac{\omega^2_{(0)}}{\omega^2}$ increases by .5 from each plot to the next.

Now these plots are gorgeous in their own right, but on some we would not immediately conclude that what we see are superpositions of lightcones.

As $\frac{\omega^2_{(0)}}{\omega^2}$ grows it becomes less likely to find a value where there are distinct lightcones; by chance, $\frac{\omega^2_{(0)}}{\omega^2} = 7.0$ is such a value and we've closely looked at this spheroid already. What we do see clearly from each plot to the next is the remission of the flat region.

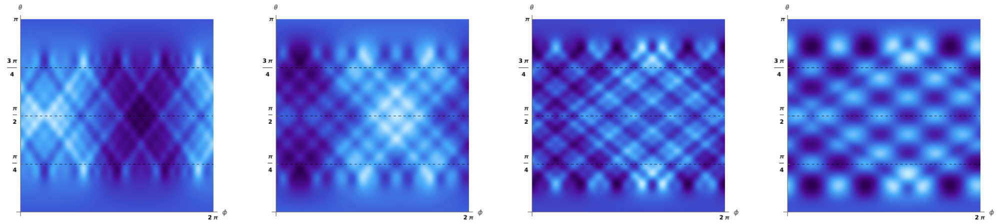

(a) $\frac{\omega^2_{(0)}}{\omega^2} = 1.5$ **(b)** $\frac{\omega^2_{(0)}}{\omega^2} = 2.0$ **(c)** $\frac{\omega^2_{(0)}}{\omega^2} = 2.5$ **(d)** $\frac{\omega^2_{(0)}}{\omega^2} = 3.0$

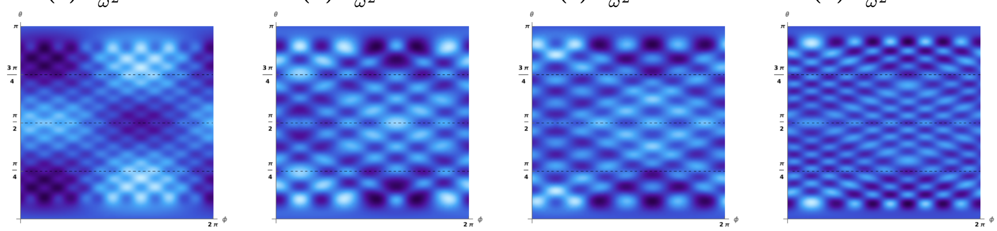

(e) $\frac{\omega^2_{(0)}}{\omega^2} = 3.5$ **(f)** $\frac{\omega^2_{(0)}}{\omega^2} = 4.0$ **(g)** $\frac{\omega^2_{(0)}}{\omega^2} = 4.5$ **(h)** $\frac{\omega^2_{(0)}}{\omega^2} = 5.0$

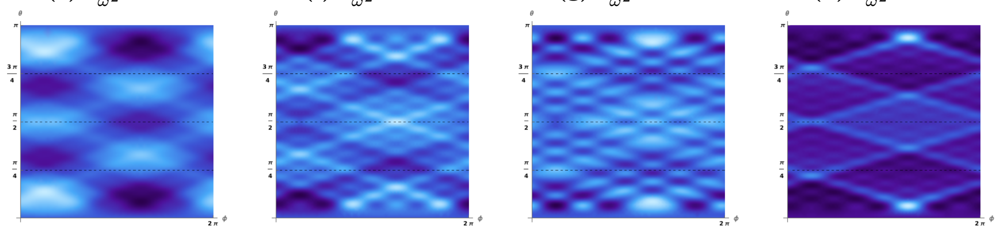

(i) $\frac{\omega^2_{(0)}}{\omega^2} = 5.5$ **(j)** $\frac{\omega^2_{(0)}}{\omega^2} = 6.0$ **(k)** $\frac{\omega^2_{(0)}}{\omega^2} = 6.5$ **(l)** $\frac{\omega^2_{(0)}}{\omega^2} = 7.0$

Figure 12: For all of these plots we sit on the equator where $\theta = \frac{\pi}{2}$. They only vary in the value chosen for the ratio $\frac{\omega^2_{(0)}}{\omega^2}$.

There are also values of $\frac{\omega^2_{(0)}}{\omega^2}$ where the plots suddenly become completely pathological: let's look at smaller distances between 1.1 and 2.5. We increase $\frac{\omega^2_{(0)}}{\omega^2}$ by .1 for each plot.

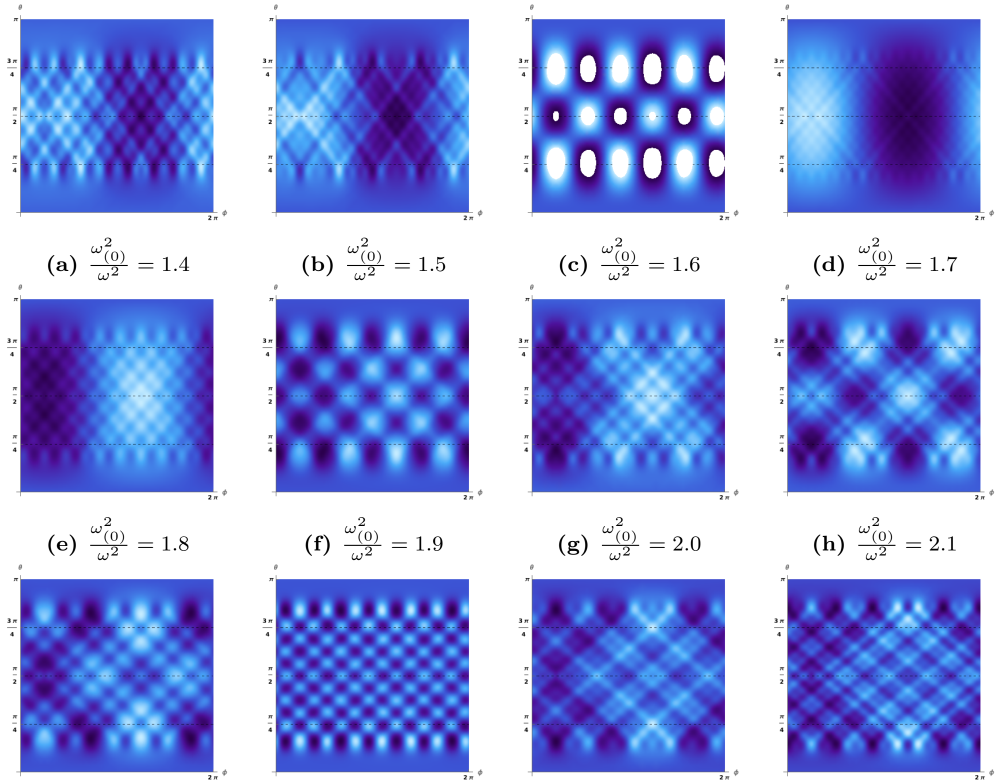

(a) $\frac{\omega^2_{(0)}}{\omega^2} = 1.4$ (b) $\frac{\omega^2_{(0)}}{\omega^2} = 1.5$ (c) $\frac{\omega^2_{(0)}}{\omega^2} = 1.6$ (d) $\frac{\omega^2_{(0)}}{\omega^2} = 1.7$

(e) $\frac{\omega^2_{(0)}}{\omega^2} = 1.8$ (f) $\frac{\omega^2_{(0)}}{\omega^2} = 1.9$ (g) $\frac{\omega^2_{(0)}}{\omega^2} = 2.0$ (h) $\frac{\omega^2_{(0)}}{\omega^2} = 2.1$

(i) $\frac{\omega^2_{(0)}}{\omega^2} = 2.2$ (j) $\frac{\omega^2_{(0)}}{\omega^2} = 2.3$ (k) $\frac{\omega^2_{(0)}}{\omega^2} = 2.4$ (l) $\frac{\omega^2_{(0)}}{\omega^2} = 2.5$

Figure 13: For all of these plots we sit on the equator where $\theta = \frac{\pi}{2}$. They only vary in the value chosen for the ratio $\frac{\omega^2_{(0)}}{\omega^2}$.

The plot for the ratio $\frac{\omega^2_{(0)}}{\omega^2} = 1.6$ sticks out. When we look at the surroundings of this region, i.e. $\frac{\omega^2_{(0)}}{\omega^2} = 1.6 \pm 0.01$ we see how fast the change from a lightcone-pattern to pathological peaks can happen. In Fig. 14 we see 3D-plots from above and from the side where the ratio $\frac{\omega^2_{(0)}}{\omega^2} = \{1.6, 1.61, 1.62\}$ respectively.

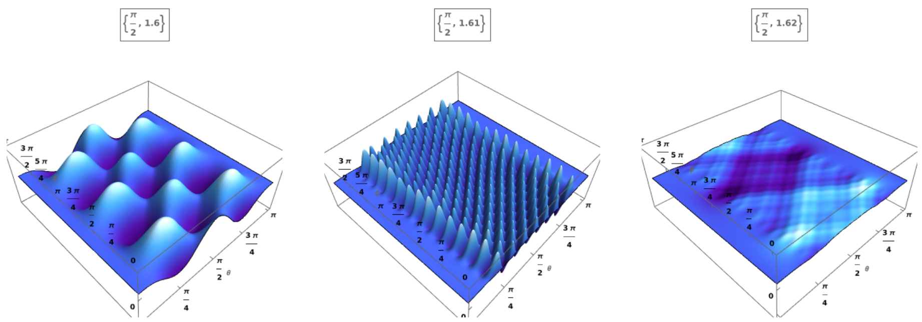

Figure 14: For all of these plots we sit on the equator where $\theta = \frac{\pi}{2}$. We see them once from above and once from the side. They only vary in the value chosen for the ratio $\frac{\omega^2_{(0)}}{\omega^2}$.

This rapid change from not seeing a lightcone pattern to seeing one is also the simple explanation as to why I've presented the values $\frac{\omega^2_{(0)}}{\omega^2} = \{1.1, 1.31, 4.95, 7.0\}$ before: For small ratio it was easy to find lightcones and the ones at $\frac{\omega^2_{(0)}}{\omega^2} = \{1.1, 1.31\}$ seemed the best visible; I've continued on to search for more by increasing the ratio $\frac{\omega_{(0)}^2}{\omega^2}$ in steps of .5 and therefore I've found lightcones close to integer values of $\frac{\omega_{(0)}^2}{\omega^2}$. This does not mean that there aren't other values for the ratio $\frac{\omega_{(0)}^2}{\omega^2}$ that display nice lightcones as well; however, it is clear that they are hard to detect by this search method when noticing that a change of .01, as it happens for $\frac{\omega_{(0)}^2}{\omega^2} = \{1.61, 1.62\}$ in Fig. 14 already changes the picture in such a significant way.

7 Appendix

These notes are based on [12], [13] and [18]. They are not meant to be a rigorous explanation of the mathematical concepts in this work. Rather, they are a compilation of my own notes and explanations that I needed to understand these concepts. When I started learning for this thesis the mathematical definitions were a source of confusion, especially because there are some concepts (between group theory, differential geometry and physics-nomenclature) that turned out to be equivalent. Therefore, these notes might help someone who starts off with the same background that I had and make it easier to read mathematicians' works.

7.1 Notes on Poisson manifolds

Already in the first chapter we say that we look at a Poisson manifold. What is that? By definition, a **Poisson manifold** is a pair $(\mathcal{P}, \pi)$ where π is a Poisson bivector field on a manifold $\mathcal{P}$. Well, what does that mean?

To have a Poisson bivector field we first need to know what a Poisson structure is. Now that is something that we see often in physics:

A **Poisson structure** on $\mathcal{P}$ is an $\mathbb{R}$-bilinear **Lie bracket** $\{\ ,\ \}$ on the space of smooth functions $\mathcal{C}^\infty(P)$ satisfying the Leibniz rule

$$\{f, gh\} = \{f, g\}h + g\{f, h\} \tag{276}$$

$\forall f, g, h \in \mathcal{C}^\infty(\mathcal{P})$ and the Jacobi identity

$$\{f, \{g, h\}\} + cycl. = 0 \tag{277}$$

Because of the Leibniz rule we can find a bivector field π:

$$\{f, g\} = \pi(df, dg) \tag{278}$$

The components of this bivector field in local coordinates $(x_1, ..., x_n)$ are

$$\pi^{ij}(x) = \{x_i, x_j\} \tag{279}$$

Therefore, to say that we look at a Poisson manifold means that we have a manifold with a Poisson structure.

If the bivector field π is invertible at each point x it is called nondegenerate or symplectic. If that is the case then we can define a symplectic form on $\mathcal{P}$. Then we have a **symplectic Poisson structure**.

We can further expand on this when we require that $\mathcal{P}$ is a finite-dimensional vector space V with coordinates $(x_1, ..., x_n)$ and define a linear Poisson structure by

$$\{x_i, x_j\} := \sum_{l \leq k \leq n} c_{ij}^k x_k \tag{280}$$

where c_{ij}^k are anti-symmetric constants.

This is what we can call a **Lie-Poisson structure**. Why? Because Eq. (280) is a Lie bracket with the structure constants c_{ij}^k, i.e., a Lie algebra g. We could even do this the other way around: a Lie algebra g with structure constants c_{ij}^k will define us a linear Poisson structure on the adjoint representation g^* through Eq. (280). We talk about the use of the word 'representation' in the next subsection.

It doesn't really matter whether we first require: "Given a Poisson manifold..." or: "Oh, I want a space on which I can use $SU(2)$!" (Which is something I would do as a physicist who wants to look at a sphere.) In the end, linear Poisson structure implies Lie algebra; and Lie algebra implies linear Poisson structure. So we call it Lie-Poisson structure.

7.2 Notes on Lie groups and Lie algebras

A Lie group G is a group that is also a differentiable manifold, i.e. the group operations of multiplication and inversion are smooth maps.

This sentence means that there is a map μ from the group into itself where two elements g_1, g_2 of the group operate as the multiplication $g_1 \cdot g_2$:

$$\mu : G \times G \to G \tag{281}$$

$$(g_1, g_2) \mapsto g_1 \cdot g_2 \tag{282}$$

and there is another map ν from the group into itself that is the inversion g^{-1} of a group element g:

$$\nu : G \to G \tag{283}$$

$$g \mapsto g^{-1} \tag{284}$$

and both the map μ and ν are smooth.

A left action $\triangleright$ of a Lie group G with elements g on a space $\mathcal{M}$ is a map

$$G \times \mathcal{M} \to \mathcal{M} \tag{285}$$

$$(g, \phi) \mapsto g \triangleright \phi \tag{286}$$

A left action simply means that the operation acts on ϕ from the left side. There are also 'right' actions. If the elements of the group were to be commutative, the left action would be the same as the right action.

In chapter 3 we use the left action $\triangleright$ when we let the elements J_i $(i = 1, 2, 3)$ of the Lie group $SU(2)$ act on a function ϕ.

We can have a group homomorphism π that is a linear transformation:

$$\pi : G \to GL(V) \tag{287}$$

where the vector space V which we use in this thesis is $V = \mathbb{C}$. π is called a representation of G. Note that π here is in group-theory-language the same thing as the bivector field π which we defined in the notes about poisson manifolds in manifold-language. This is due to the fact that Lie groups are characteristically a group *and* a differentiable manifold, which is also what makes them so very useful.

Given a Lie group G and generators $T^1, ..., T^n$ of the group we can take the set of the generators as a basis and relate them by a linear combination; for us the latter is given by the commutation relations. The basis spans an n-dimensional vector space; giving that space the commutation relations makes it a Lie algebra $\mathfrak{g}$. The commutation relations satisfy the Leibniz rule and Jacobi identity – we've seen this already when we defined the Poisson structure.

In short, the nomenclature is: $T^1, ..., T^n$ are the *generators* of the Lie group G and the set of these generators are the *basis* of the Lie algebra $\mathfrak{g}$.

What do we know about the commutation relations?

Let $\mathfrak{g}$ be a finite dimensional Lie algebra and let $T^1, ..., T^n$ be a basis for $\mathfrak{g}$, then $\forall a, b$:

$$[T^a, T^b] = \sum_{k=1}^{n} f^{abc} T_c \tag{288}$$

where f^{abc} are called structure constants. We've seen this in manifold-language as well when we defined a Lie-Poisson structure.

The structure constants are antisymmetric and obey the Jacobi identity

$$f^{ade} f^{bcd} + f^{bde} f^{cad} + f^{cde} f^{abd} = 0 \tag{289}$$

which can be found from the commutation relations and the identity

$$[T^a, [T^b, T^c]] + [T^b, [T^c, T^a]] + [T^c, [T^a, T^b]] = 0 \tag{290}$$

We are interested in compact, simple Lie groups. *Compact* means that the Lie group has a finite number of generators. *Simple* means: there is no generator that commutes with all others (and we are looking for non-commutativity after all!), which you might know to be called 'Non-Abelian', and additionally it is not possible to divide the Lie algebra into distinct sets of generators.

Let us now move on to less theoretical concepts; Now let's look at some specific groups!

The general linear group of $N \times N$ matrices (i.e. linear transformations) denoted by $GL(N, \mathbb{C})$ consists of all $N \times N$ invertible complex matrices together with matrix multiplication as the group operation.

$$GL(N, \mathbb{C}) := \{A \in Mat(N, \mathbb{C}); \det A \neq 0\} \tag{291}$$

It is a group because we have an inverse element – the matrices are invertible – and the identity matrix as the identity element of the group.

We can take a subgroup of this group, i.e. only those matrices that are unitary as well. This is the group $U(N)$ where U stands for unitary.

$$U(N, \mathbb{C}) := \{A \in Mat(N, \mathbb{C}); AA^\dagger = \mathbb{I}, \det A \neq 0\} \tag{292}$$

$$U(N, \mathbb{C}) \subseteq GL(N, \mathbb{C}) \tag{293}$$

Take another subgroup and we arrive at the Special Unitary group $SU(N, \mathbb{C})$. Not only are these matrices unitary but they are called *special* meaning that they all have determinant 1.

$$SU(N, \mathbb{C}) := \{A \in Mat(N, \mathbb{C}); AA^\dagger = \mathbb{I}, \det(A) = 1\} \tag{294}$$

$$SU(N, \mathbb{C}) \subseteq U(N, \mathbb{C}) \subseteq GL(N, \mathbb{C}) \tag{295}$$

This group has dimension

$$\dim(SU(N,\mathbb{C})) = N^2 - 1 \tag{296}$$

From now on we will write just $SU(N)$ instead of $SU(N,\mathbb{C})$ because in this thesis we always use matrices with complex entries. Sometimes in physics we use $SU(N)$ to denote the Lie *algebra*, not the group. To distinguish between them we adopt the mathematicians' convention and use $SU(N)$ with capital letters to denote the group and $su(N)$ with small letters for the algebra.

The Lie algebra $su(N)$ can be defined by

$$su(N) := \{A \in gl(N); A^\dagger = -A, \mathrm{Tr}(A) = 0\} \tag{297}$$

where $gl(N)$ means the general linear algebra (associated with $GL(N)$ from above), i.e. $N \times N$ matrices accompanied by commutation relations.

We could identify the Lie algebra $su(N)$, and you will see this in some references, with the set of traceless anti-Hermitian $N \times N$ complex matrices and with the regular commutator as a Lie bracket. In physics we use the (equivalent) representation: The set of traceless Hermitian $N \times N$ complex matrices with Lie bracket given by $-i$ times the commutator.

We use the group $SU(N)$ and algebra $su(N)$ a number of times in physics. Here we are interested in $SU(2)$: the unitary traceless 2×2 matrices. Most of us know these as the Pauli matrices (but keep in mind that this is the physicists' representation).

7.3 SU(2)

The group $SU(2)$ is the group of 2-dimensional matrices which are unitary and have determinant 1. In physics the chosen representation is some multiple of the Pauli matrices:

$$\sigma_1 = \begin{pmatrix} 1 & 0 \\ 0 & 1 \end{pmatrix} \qquad \sigma_2 = \begin{pmatrix} 0 & -i \\ i & 0 \end{pmatrix} \qquad \sigma_3 = \begin{pmatrix} 1 & 0 \\ 0 & -1 \end{pmatrix} \tag{298}$$

Most often the generators of the group are called J_a (sometimes L instead of J) and given by:

$$J_a = \frac{\sigma_a}{2} \tag{299}$$

The commutation relations are therefore simply given by

$$\mathrm{Tr}[J_a, J_b] = i\epsilon_{abc} J_c \tag{300}$$

$$\tag{301}$$

where like indices are summed and ϵ_{abc} is the Levi-Civita symbol.

The matrices used for fuzzy spheres are merely a linear transformation of these (i.e. another representation of $su(2)$).

We also use the Casimir operator of $su(2)$ to characterise our sphere. A Casimir operator can be found for all Lie algebras (sometimes there is more than one) and is a polynomial of the generators which commutes with all generators.

$$\vec{J}^2 = (J_1)^2 + (J_2)^2 + (J_3)^2 \tag{302}$$

$$[\vec{J}^2, J_i] = 0 \tag{303}$$

The Casimir operator is also a multiple of the identity matrix.

$$\vec{J}^2 = c_R \mathbb{I} \tag{304}$$

for the representation of $su(2)$ that we use here, the constant c_R is given by:

$$c_R = \frac{1}{4}(N^2 - 1) \tag{305}$$

The factor $N^2 - 1$ is the dimension of the group and the factor $\frac{1}{4}$ is due to the particular choice of representation.

These notes and the knowledge about the use of angular momentum operators in physics that readers of this thesis probably have should be sufficient to understand the use of the Lie algebra $su(2)$ throughout the thesis.

Bibliography

[1] John D. Norton. "How Hume and Mach Helped Einstein Find Special Relativity". In: 2004.

[2] Badis Ydri. "Lectures on Matrix Field Theory I". In: *arXiv: High Energy Physics - Theory* (2016).

[3] Harold C Steinacker. "Non-commutative geometry and matrix models". In: *arXiv: High Energy Physics - Theory* (2011).

[4] Marco Maceda. "Fuzzy Physics: A Brief Overview of Noncommutative Geometry in Physics". In: 2011.

[5] John Madore. "The Fuzzy sphere". In: *Classical and Quantum Gravity* 9 (1992), pp. 69–87.

[6] Badis Ydri. "Fuzzy Physics". In: 2001.

[7] Shiraz Minwalla, Mark Van Raamsdonk, and Nathan Seiberg. "Noncommutative perturbative dynamics". In: *Journal of High Energy Physics* 2000 (2000), pp. 020–020.

[8] Richard Joseph Szabo. "Quantum field theory on noncommutative spaces". In: *Physics Reports* 378 (2001), pp. 207–299.

[9] Arturo Echeverría-Enríquez et al. "Mathematical Foundations of Geometric Quantization". In: *arXiv: Mathematical Physics* (1998).

[10] Aiyalam P. Balachandran, Seckin Kurkcuoglu, and Sachindeo Vaidya. "Lectures on Fuzzy and Fuzzy Susy Physics". In: 2005.

[11] Garnik G. Alexanian, Aleksandr Pinzul, and Allen Stern. "Generalized coherent state approach to star products and applications to the fuzzy sphere". In: *Nuclear Physics* 600 (2001), pp. 531–547.

[12] Nima Moshayedi. "Lectures on Symplectic Geometry, Poisson Geometry, Deformation Quantization and Quantum Field Theory". In: 2020.

[13] Matthias Blau. "Symplectic Geometry and Geometric Quantization". In: 2020.

[14] Badis Ydri, Rouag Ahlam, and Ramda Khaled. "Emergent fuzzy geometry and fuzzy physics in four dimensions". In: *Nuclear Physics* 916 (2017), pp. 567–606.

[15] Harold C Steinacker. "Gravity as a quantum effect on quantum space-time". In: *Physics Letters B* (2022).

[16] A. Chaney, Lei Lu, and Allen Stern. "Lorentzian fuzzy spheres". In: *Physical Review D* 92 (2015), p. 064021.

[17] Harold C Steinacker. "Cosmological space-times with resolved Big Bang in Yang-Mills matrix models". In: *Journal of High Energy Physics* 2018 (2017), pp. 1–24.

[18] Michael E. Peskin and Daniel V. Schroeder. "An Introduction To Quantum Field Theory". In: 1995.

[19] Walter A. Strauss. "Partial Differential Equations: An Introduction". In: 1992.

[20] Michael V. Sadovskii. "Quantum Field Theory". In: 2013.

[21] Matthias Blau. "Lecture Notes on General Relativity". In: 2017.